10
Radiationless Transitions

J. JORTNER and S. MUKAMEL
Tel-Aviv University

Dedication

This article is dedicated to the memory of Charles Coulson.

10.1 INTRODUCTION

In order to classify the diverse field of radiationless transitions let us first adopt the experimentalist's point of view and specify a radiationless process in terms of 'transitions' between 'states' (i.e. electronic, vibrational or rotational) of a system (i.e. an atom, a molecule or a solid) which do not involve absorption or emission of radiation. Such a broad definition encompasses a wide class of physical and chemical phenomena, which can be classified in the following manner:

A. *Relaxation in atoms*
  (A1) Atomic Autoionisation[1]

B. *Relaxation in molecules*
  a. *Basic processes*
    (B1) Molecular Autoionisation[2]
    (B2) Predissociation[2,3]
    (B3) Electronic relaxation between different states of a large molecule. Internal conversion (spin conserving processes) and intersystem crossing (involving pure spin states of different spin multiplicity)[4-16]
  b. *Medium induced processes*
    (B4) Vibrational relaxation[17]
    (B5) Thermally induced predissociation[18]
  c. *Complex processes*
    (B6) Photochemical rearrangements[19-21]

C. *Relaxation in solids*
  (C1) Thermal ionisation of impurities[22]
  (C2) Thermal electron capture[22]
  (C3) Electronic relaxation in impurity states
  (C4) Electron energy transfer[23-25]
  (C5) Autoionisation of metastable excitons[26]
  (C6) Electronic relaxation of excited states[26]

D. *Relaxation in solutions*
  (D1) Thermal electron transfer[27]
  (D2) Electronic energy transfer[23]
  (D3) Dynamics of electron localisation[28]

From the theoretician's point of view such a broad definition involves some hidden assumptions and pitfalls. First, the concept of a 'state of the system' has to be properly characterised. The experimental excitation conditions by optical, electron impact, collisional or thermal excitation have to be precisely

defined in order to specify the nature of the non-stationary state of the system which exhibits time evolution. Second, one has to consider not 'transitions' in the general vague sense but rather focus attention on channels of the molecular system. From this point of view the main decay channels in excited molecular states can be classified as follows:

(*a*) Radiative decay.
(*b*) Direct decomposition, i.e. photodissociation and photoionisation.
(*c*) Indirect decomposition, i.e. predissociation and autoionisation.
(*d*) Non-radiative electronic relaxation in excited states of large molecules.
(*e*) Vibrational relaxation.
(*f*) Unimolecular photochemical rearrangement reactions.

Processes (*a*)–(*c*) obviously occur in an 'isolated', collision free, molecule. Process (*d*) also takes place in an isolated large molecule which corresponds to the 'statistical limit'[29-31], while it may be induced by medium perturbations in a small molecule[32-34]. Process (*e*) exclusively originates from medium perturbations[17]. Processes of type (*f*) are very complex[21] and may involve a combination of processes (*b*)–(*d*).

The large bulk of experimental information now available on the radiative decay characteristics and the emission quantum yields from electronically excited molecular states[6-16, 35-40] does not only provide information concerning the radiative decay channels but involves as 'hidden variables' the contributions of other non-radiative decay channels. A major goal of the theory is to untangle this information and to provide a comprehensive picture of radiationless processes in electronically excited molecular states, which will emerge from a proper description of their radiative decay. Complementary information will be obtained from the analysis of optical lineshape data and from the quantum yields for the population of non-radiative decay channels. It is the purpose of this review to discuss the aspects of recent theoretical work which elucidate the interplay between various radiative and non-radiative decay channels in electronically excited states of polyatomic molecules, thus providing a unified theoretical picture regarding the fate of bound, electronically excited, states of large molecules[29-34, 41-74]. This review is not intended to be exhaustive or complete, but rather to expose the current understanding of the important class of electronic relaxation phenomena.

10.2 'SHORT TIME' AND 'LONG TIME' EXCITATION EXPERIMENTS

From the experimentalist's point of view the following spectroscopic information is of fundamental importance for the elucidation of the decay characteristics of excited molecular states.

(1) Decay characteristics of electronically excited states. The most detailed information originates from the time- and energy-resolved pattern of the radiative decay of excited electronic states. In the simplest case the decay pattern is exponential and the excited state is characterised by a single lifetime. More complex decay patterns which involve a superposition of exponentials were also recorded. Finally, the decay may (in principle) exhibit an oscillatory

behaviour which originates from interference between closely spaced discrete levels. This phenomenon of quantum beats, which is well known in level crossing atomic spectroscopy[76], is not yet experimentally established in large molecules.

(2) Time evolution of the population of molecular excited states other than those which were initially excited. In particular, we are interested in the population of molecular states which act as exit channels in predissociation and in electronic relaxation.

(3) Cross sections for photon scattering from molecules. These involve both elastic photon scattering to the ground electronic-vibrational state and resonance Raman scattering of the ground electronic configuration. We shall refer to these processes as 'resonance fluorescence'.

(4) Optical absorption lineshapes.

(5) Cross sections for photofragmentation of molecules undergoing direct photodissociation.

(6) Cross sections for populations of exit channels in predissociation and for electronic relaxation.

(7) Quantum yields for resonance fluorescence.

(8) Quantum yields for photodissociation and predissociation.

These experimental observables fall into two different categories. In general, two classes of experiments, which will be referred to as 'short excitation' and 'long excitation' processes, can be utilised to extract physical information concerning the decay of electronically excited states of large molecules. When the temporal duration of the exciting photon field is short relative to the reciprocal width of the molecular resonance, it is feasible to separate the excitation and the decay processes and to consider the decay pattern of the metastable state[10,30,31,41,42,64,71,75-79]. This experimental approach involves a 'short excitation' process. The study of the decay pattern of an 'initially' excited state corresponds to such a 'short excitation' experiment. On the other hand, when the exciting photon field is characterised by a high-energy resolution, being switched on for long periods (relative to the decay time), the excitation and the decay processes cannot be separated and one has to consider resonance scattering from large molecules within the framework of a single quantum mechanical process. Such 'long excitation' experiments involve the determination of optical line shapes, cross sections for resonance fluorescence, for intramolecular electronic relaxation and for photodissociation[66,71,72-76,80]. Emission quantum yields can be obtained both from 'short time' excitation experiments, by the integration of the decay curve or from 'long time' experiments, which result in the energy dependence of the quantum yield. In general, the physical information extracted from 'short time' and 'long time' excitation experiments is complementary but not identical[71].

10.3 BASIC MODELS AND BASIS SETS

Several theoretical models for the decay characteristics of electronically excited states have been advanced and solved at various levels of sophistication. Such models provide a schematic description of the energy levels of the

zero order Hamiltonian, which should incorporate both the molecular system and the radiation field, while the residual interaction couples the zero order states. Clearly, the choice of the basis set is a matter of convenience and does not affect observable quantities. To obtain a transparent physical picture, which will provide a basis for numerical calculations, the selection of the zero order states has to satisfy two basic criteria: (i) the energies of the basis states have to be as close as possible to the spectroscopic energy levels; (ii) one would like to be able to employ a moderately small, truncated, basis set incorporating only a limited number of excited electronic configurations. Let us consider now the conventional dissection of the Hamiltonian, H, for a system consisting of a molecule which interacts with the radiation field:

$$H = H_M + H_{rad} + H_{int} \tag{10.1}$$

where the total molecular Hamiltonian, H_M, consists of a zero order molecular Hamiltonian H_{MO}, and the non-adiabatic intramolecular interaction, H_V, which involves interstate coupling via the nuclear kinetic energy or spin–orbit coupling. Thus the molecular Hamiltonian is

$$H_M = H_{MO} + H_V \tag{10.2}$$

To complete the definitions in equation (10.1), H_{rad} is the Hamiltonian for the free radiation field while H_{int} labels the radiation–matter interaction term.

Following the work of Franck and Sponer[81] in molecular physics and of Kubo[82] in solid state physics, it was widely accepted that a proper choice of the zero order states involves the Born–Oppenheimer (BO) representation[83-86], whereupon the nuclear kinetic energy operator provides the coupling term for internal conversion. There has recently been a lively controversy regarding the nature of these interactions and several authors have confronted the Herzberg–Teller[84,86] coupling with the breakdown of the BO approximation. We shall now demonstrate that the utilisation of the BO basis set minimises off-resonance coupling terms between different electronic configurations, by discussing the general features and merits of the adiabatic BO basis and the crude adiabatic[84] basis set.

The electronically excited eigenstates of the zero order Hamiltonian, H_{MO}, which is not yet specified, are labelled as follows:

(1) Discrete vibronic levels $|s\rangle$, $|r\rangle$, etc., of an excited electronic configuration.

(2) A manifold of levels $\{|l\rangle\}$ corresponding to a lower electronic configuration and which are quasi-degenerate with the $|s\rangle$ (and/or to the $|r\rangle$) level.

(3) Other bound zero order states $\{|b\rangle\}$ which correspond to vibronic components of different electronic configurations and which are well separated from $|s\rangle$ (and $|r\rangle$ etc.) relative to their total width. In fact, when $|s\rangle$ and $|r\rangle$ in (1) are coarsely spaced, $|r\rangle$ can be taken within the $|b\rangle$ states which can also include different vibronic components of the same electronic configuration as $|s\rangle$. In general, the levels of types (1), (2) and (3) portrayed in Figure 10.1 are sufficient for the description of non-reactive electronic relaxation. The electronic ground state is labelled by the vibronic components $|g\,v\rangle$ where $v = 0$ refers to the vibrationless level. It is important to notice that the low-lying ground states $|g\,v\rangle$ can be considered as eigenfunctions of

H_{M0} as well as of H_M, as off-resonance non-adiabatic corrections for these states are negligible

Consider now the dissection of the molecular Hamiltonian H_M T_Q $T_r + U(r,Q)$, where r and Q represent electronic and nuclear coordinates. T represents the kinetic energy operator and $U(r,Q)$ is the potential energy.

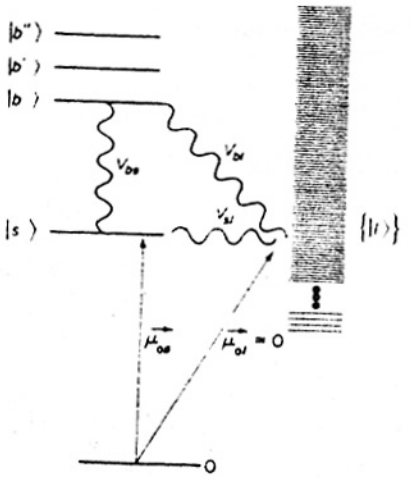

Figure 10.1 A schematic representation of the relevant molecular states and couplings. Wavy lines represent intramolecular coupling. Arrows indicate dipole coupling via the interaction with the radiation field

Let $\{|nv\rangle\}$ be any complete set of molecular zero order functions where the electronic and the nuclear motion has been arbitrarily separated. The first index refers to the electronic state and the second to the vibrational state. We can then define the projection operator $\hat{P}_{nv} = |nv\rangle\langle nv|$. Utilising the completeness relation $\sum_{n,v} \hat{P}_{nv} = 1$, and the resulting trivial relation $H_M = \sum_{n,v} \hat{P}_{nv} H_M \sum_{n,v} \hat{P}_{n,v}$ we can then define the components of equation (10.2) via

$$H_{M0} = \sum_{n,v} \hat{P}_{nv} H_M \hat{P}_{nv}$$
$$H_V = \sum_{nv} \sum_{\substack{n'v' \\ nv \neq n'v'}} \hat{P}_{nv} H_M \hat{P}_{n'v'} \qquad (10.3)$$

We shall now consider the adiabatic (A) and crude adiabatic (CA) basis sets[84] assuming that each set is complete for any value of Q, noting in passing that it can easily be demonstrated that a molecular function can be expanded in terms of either the (orthonormal) adiabatic or the crude adiabatic set. This is, however, a necessary but not a sufficient condition for completeness.

In the Born-Oppenheimer representation $|nv\rangle = \phi_n^A(r,Q)\chi_{nv}^A(Q)$ where the electronic ϕ_n^A and nuclear χ_{nv}^A wave functions satisfy the well known equations

$$[T_r + U(r,Q)]\phi_n^A(r,Q) = E_n^{(A)}(Q)\phi_n^A(r,Q)$$
$$[T_Q + E_n^{(A)}(Q) + \langle\phi_n^A|T_Q|\phi_n^A\rangle]\chi_{nv}^A(Q) = E_{nv}^A\chi_{nv}^A(Q) \qquad (10.4)$$

so that

$$H_{MO}^{(A)} = \sum_{nv} |\phi_n^A \chi_{nv}^A\rangle E_{nv}^A \langle \phi_n^A \chi_{nv}^A| \tag{10.5a}$$

while

$$H_V^{(A)} = \sum_{nv} \sum_{\substack{n'v' \\ \neq nv}} |\phi_n^A \chi_{nv}^A\rangle \left\{ \left(\chi_{nv}^A \middle| \frac{\langle \phi_n^A | \hat{c} U / \hat{c} Q | \phi_{n'}^A \rangle \hat{c}}{E_n(Q) - E_{n'}(Q)} \hat{c} Q \middle| \chi_{n'v'}^A \right) \right.$$

$$\left. + \tfrac{1}{2} (\chi_{nv}^A | \langle \phi_n^A | \hat{c}^2 / \hat{c} Q^2 | \phi_{n'v'}^A \rangle | \chi_{n'v'}^A) \right\} \langle \phi_n^A \chi_{n'v'}^A | \tag{10.5b}$$

where $\langle\ \rangle$ denotes integration in the electronic r space, while $(\ )$ denoted the integration in the nuclear Q space. In the crude adiabatic representation[84] $|nv\rangle = \phi_n^{CA}(r,Q_0)\chi_{nv}^{CA}(Q)$, where the electronic ϕ^{CA} and nuclear χ^{CA} wave functions satisfy

$$[Tr + U(r,Q_0)]\phi_n^{CA} = E_n^{(A)}(Q_0)\phi_n^{CA}$$

$$[T_Q + E_n^{CA}(Q_0) + \langle \phi_n^{CA} | \Delta U(r,Q) | \phi_n^{CA} \rangle] \chi_{nv}^{CA}(Q) = E_{nv}^{CA} \chi_{nv}^{CA}(Q) \tag{10.6}$$

where $\Delta U = U(r,Q) - U(r,Q_0)$ and Q_0 is an arbitrary fixed nuclear configuration. In this representation

$$H_0^{CA} = \sum_{nv} |\phi_n^{CA} \chi_{nv}^{CA}\rangle E_{nv}^{CA} \langle \phi_n^{CA} \chi_{nv}^{CA}| \tag{10.7a}$$

$$V^{CA} = \sum_{nv} \sum_{\substack{n'v' \\ \neq nv}} |\phi_n^{CA} \chi_{nv}^{CA}\rangle (\langle \phi_n^{CA} \chi_{nv}^{CA} | T_Q + \Delta U(r,Q) | \phi_{n'}^{CA} \chi_{n'v'}^{CA} \rangle) \langle \phi_{n'}^{CA} \chi_{n'v'}^{CA}| \tag{10.7b}$$

Equations (10.6) and (10.7) provide a self-consistent definition of the zero order Hamiltonian of both basis sets. The following remarks should be made at this point.

(1) Both A and CA untruncated basis sets are, of course, adequate from the formal point of view.

(2) Both the A and CA basis sets are diagonal within the same electronic configuration. This point is well known concerning the A basis[84], while regarding the CA basis it constitutes a special case of the prediagonalisation conditions discussed by Hobey and McLachlan[98].

(3) While the adiabatic potential surfaces $E_n^{(A)}(Q)$ are well known from theoretical calculations, until recently no information was available concerning the crude adiabatic potential surfaces $E_n^{(CA)}(Q) = \langle \phi_n^{CA} | \Delta U(r,Q) | \phi_n^{CA} \rangle$. The validity of the CA wave function for representing the energy levels of diatomics was examined by Lefebvre *et al.*[96] for the ground state of H_2 and N_2. From their results reproduced in Table 10.1 it is apparent that the CA procedure pays a heavy toll for not allowing the electron distribution to adjust to the nuclear configurations. The CA wave functions lead to poor zero-point energies in the case of H_2 while for the case of N_2 the resemblance between the A and the CA potential surfaces is merely accidental. An intermediate procedure[96], labelled as the semi-CA approach, which relaxes the electronic freedom for the core electrons, somewhat improves the situation but still leads to poor results. One can thus conclude that the CA basis results in an extremely poor representation of the 'spectroscopic' molecular

Table 10.1 Zero-point ground-state energies for adiabatic (A) and crude-adiabatic (CA) potential surfaces of diatomics*

Molecule	*Zero point energy* cm^{-1}	*Method*
H_2	2 639	(A) 1s and $2p_\sigma$ basis
	4 179	(CA) 1s and $2p_\sigma$ basis
	2 168	Experiment
N_2	1 434	(A) Minimum basis set
	1 465	(A) Double-ζ basis
	21 826	(CA) Minimum basis set
	4 320	Semi (CA) Double-ζ set
	1 176	Experiment

* Data from Atabek, Hardisson and Lefebvre (1973). *Chem. Phys. Lett.*, **20**, 40

states, thus violating our basic conditions (i). This constitutes a serious difficulty involved in using the (CA) basis.

(4) The conventional Condon approximation, which is popular in the study of radiative coupling terms in polyatomics and in solids, is inadequate for the evaluation of interstate coupling terms originating from the breakdown of the BO approximation. The Condon approximation applied to the matrix elements in equation (10.5b) involves the following simplifications: (*a*) The second term in (10.5b) is discarded. (*b*) The energy denominator $E_n(Q) - E_{n'}(Q)$ is assumed to be weakly dependent on the nuclear coordinates and is set to be equal to a constant, say the electronic energy gap, ΔE, between the origins of the electronic configurations $|n\rangle$ and $|n'\rangle$. (*c*) The electronic matrix elements $\langle \phi_n^{(A)} | \partial U / \partial Q | \phi_{n'}^{(A)} \rangle$ are assumed to be slowly varying functions of the nuclear configurations, being taken at Q_0, say the equilibrium configuration of one state. We note in passing that assumptions (*b*) and (*c*) provide necessary conditions for the validity of assumption (*a*) as each of the matrix elements in (10.5b) does not involve a Hermitian operator. Provided that assumptions (*b*) and (*c*) hold the interstate coupling matrix elements are

$$(\tilde{H}_V^{(A)})_{n\nu,n'\nu'} = \frac{\langle \phi_n(r,Q_0) | (\partial U/\partial Q)_{Q_0} | \phi_{n'}(r,Q_0) \rangle}{\Delta E} \times \left\{ \chi_{n\nu}(Q) \left| \frac{\partial}{\partial Q} \right| \chi_{n\nu}(Q) \right\} \tag{10.8}$$

being factored into an electronic matrix element, which for small displacements is non-vanishing only for some promoting modes[48,57,99], Q_x, and a Franck–Condon vibrational overlap factor. It has been known from work on relaxation in solids[100] and molecular predissociation[101] that the Condon approximation is invalid for non-adiabatic interstate coupling, and that the major contribution to the integrals in (10.5b) originates from the vicinity of the crossing hypersurface of the multi-dimensional potential curves. The Feynman operator technique was applied[57] to evaluate the interstate coupling matrix elements in (10.5b). The formal results could be disentangled[57] only for the case of a two-electronic-level system in the weak electronic-vibrational coupling limit[47,48] [i.e. a small relative displacement between the minimum

positions of the two electronic potential surfaces $E_n(Q)$ and $E_{n'}(Q)$]. This is a situation common for electronic relaxation in large organic molecules (see Section 10.13). The interstate coupling takes the form

$$(H_V^{(A)})_{nv,n'v'} = (\tilde{H}_V^{(A)})_{nv,n'v'}\zeta \tag{10.9}$$

which is just the Condon approximation, equation (10.8), modified by a correction factor. Detailed numerical calculations[57] of ζ are displayed in Figure 10.2, for both resonance and for off-resonance coupling. For near-resonance coupling a reasonable approximation is $\zeta \propto \Delta E/\hbar\bar{\omega}$, where $\bar{\omega}$

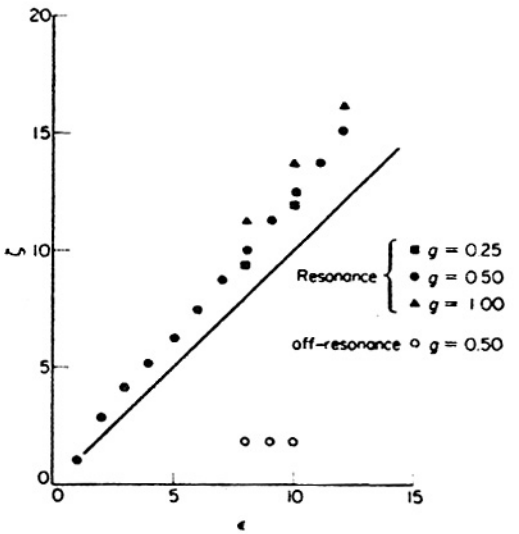

Figure 10.2 The non-Condon correction factor ζ for non-adiabatic interstate coupling. The reduced energy is $\varepsilon = \Delta E/\hbar\bar{\omega}$ expressed in terms of the electronic energy gap ΔE and the mean molecular frequency. The electron–phonon coupling strength $g = \sum_i (\Delta_i^2/2)$ is expressed in terms of the reduced displacements Δ_i between the minima of the potential surfaces normalised to the nuclear zero-point r.m.s. displacement

is the mean molecular vibrational frequency. Thus $(\tilde{H}_V^{(A)})_{nv,n'v'} \propto \Delta E^{-1}$ while $\zeta \propto \Delta E/\hbar\bar{\omega}$, whereupon the strength of near-resonance coupling is practically independent of the energy gap. We further notice only a weak dependence of ζ on the (weak) electron–phonon coupling strengths. On the other hand, for off-resonance coupling $\zeta \approx 1$–2, being practically independent of ΔE, so that $(H_V^{(A)})_{nv,n'v'} \propto 1/\Delta E$, which results in small correction terms originating from interstate coupling between $|s\rangle$ and $|b\rangle$ or $|l\rangle$ and $|b\rangle$ in Figure 10.1. The BO basis minimises off-resonance coupling terms between different electronic configurations.

(5) The situation is drastically different with regard to the CA basis where the near-resonance and off-resonance coupling terms assume the same form.

The ratio of the off-resonance coupling terms in the A and in the CA basis is of the order $\hbar\bar{\omega}\ \Delta E \sim 0.1$.

The last point illustrates the major difficulty associated with the use of the CA basis to describe intramolecular coupling and intramolecular relaxation. The contributions of the off-resonance interstate coupling, which always exist in real life, cannot be disregarded, whereupon a large number of (CA) electronic configurations has to be incorporated to account properly for the features of intramolecular electronic relaxation, thus violating the basic convenience condition (ii) for the choice of a basis set. The utilisation of the BO basis and the identification of H_v with the breakdown of the BO approximation provides the mathematical basis for the basic model system for intramolecular electronic relaxation which involves two electronically excited configurations, as portrayed in Figure 10.3.

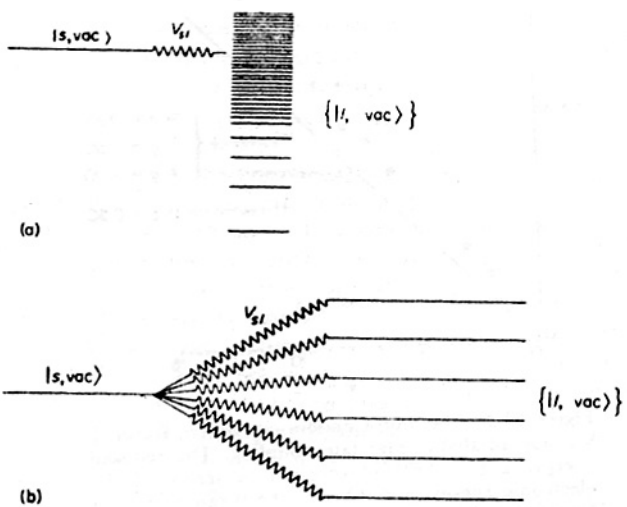

Figure 10.3 Basic models for intramolecular electronic relaxation in a large molecule (a), and for interstate coupling in a small molecule (b)

Apart from the nuclear kinetic energy terms which scramble zero order BO states of the same spin multiplicity, other intramolecular interaction terms may modify the mixing. For example, electronic–rotational interactions between spin states of the same multiplicity may be considered. These coupling matrix elements which conserve the rotational quantum number K (for a symmetric top) are of the order[102] $|K^2\hbar^4/I^2\Delta E|$ where I is the appropriate moment of inertia. Such contributions[102] are expected to be small relative to the resonance vibronic type coupling terms. Obviously, spin–orbit interactions have to be included in the case of mixing of quasi-degenerate pure spin BO vibronic levels which correspond to two electronic states of different spin multiplicity[5, 103-105]. This problem has been quite extensively surveyed in the recent literature and we shall refrain from reviewing it.

In most work on the theory of intramolecular coupling and electronic relaxation in large molecules the role of rotational effects was disregarded. Concerning small molecules, we should like to mention rotational effects on interstate coupling in diatomics, originating from the change in the rotational constant between two electronic states, which modifies the energy separation between these rotovibronic levels[106]. More interesting is the marked dependence of the predissociation rates of some diatomics on the rotational quantum number which is due to vibrational–rotational coupling effects[107,108]. In the case of large molecules we argue qualitatively that vibrational–rotational coupling effects are expected to be small, whereupon interstate coupling conserves the rotational quantum numbers, and one can thus just consider vibrational rather than roto-vibrational manifolds corresponding to different electronic configurations. A complete theoretical study of this problem would be of interest. From the experimental point of view the work of Parmenter and Schuh[109] on resonance fluorescence from the first singlet state of benzene has demonstrated that intersystem crossing in a large molecule is insensitive to rotational effects. An attempt was recently made[110] to interpret the fast pressure-independent intersystem crossing from the lowest triplet in aromatic hydrocarbons in the low-pressure gas by invoking the role of rotational effects. Unfortunately, no distinction was made[110] between inhomogeneous line broadening and homogeneous broadening. The latter results in intramolecular relaxation while rotational effects contribute to the former width and not to intramolecular decay.

The highly idealised level scheme in Figure 10.3 provides a universal model for interstate coupling in polyatomics and for radiationless transitions in a large 'isolated' molecule. A zero order vibronic level $|s\rangle$ of a higher electronic state, which carries all the oscillator strength from the ground state, is quasi-degenerate with an intramolecular manifold $\{|l\rangle\}$ of bound levels which correspond to a lower electronic state. The $\{|l\rangle\}$ manifold is devoid of oscillator strength. In the case of a large molecule, when the energy gap between the electronic origins of $|s\rangle$ and the $\{|l\rangle\}$ states is reasonably large ($\sim$1 eV), we have large densities of $\{|l\rangle\}$ states which are quasi-degenerate with $|s\rangle$. Typical examples for total density of states are given in Table 10.2. Although only a subset of levels in the $\{|l\rangle\}$ manifold is effectively coupled to $|s\rangle$, the density of these strongly coupled background levels in many large molecules is still overwhelmingly large. The $|s\rangle$ state plays a central role as it

Table 10.2 Total densities of vibronic background states in some organic molecules as calculated from the harmonic model

Molecule	*Lower state*	*Upper state*	ΔE/cm^{-1}	ρ/cm
Anthracene	$T_1(^3B_{2u})$	$S_1(^1B_{2u})$	12 000	5×10^{10}
Naphthalene	$S_0(^1A_g)$	$T_1(^3B_{2u})$	20 000	8×10^{15}
Azulene	$S_0(^1A_1)$	$S_0(^1B_1)$	14 000	10^{11}
Benzene	$T_1(^3B_{1u})$	$S_1(^1B_{2u})$	8 400	8×10^{4}
Naphthalene	$S_1(^1B_{3u})$	$S_2(^1B_{2u})$	3 400	2×10^{3}
Benzophenone	T_1	S_1	2 800	10^{3}

is optically accessible from the ground state. The situation is analogous to a 'doorway state' in nuclear scattering where a single excitation can be reached via the incident channel[111, 112]. This physical system will not exhibit a truly intramolecular non-radiative relaxation[30] but rather practical irreversible decay on the time scale of interest[30]. Subsequent consecutive damping processes (which were disregarded in this simple scheme) of the $\{|l\rangle\}$ manifold, such as infrared radiation, or photon emission in the case of internal conversion, will deplete these levels (see Section 10.11), ensuring the occurrence of irreversible intramolecular radiationless processes in an isolated large molecule. This situation is commonly referred to as the statistical limit.

The flexibility of molecular systems allows us to change the density of the $\{|l\rangle\}$ background states at will, by considering different molecules characterised by different numbers of vibrational degrees of freedom and by varying the electronic energy gap (see Table 10.2 and Figure 10.3b). In this context one has to be careful to distinguish between the implications of interstate coupling and intramolecular relaxation. Intramolecular interstate non-adiabatic coupling is exhibited both in 'small' and in 'statistical' molecules. In small molecules[113] where the level density of the background states is low, no intramolecular relaxation is encountered.

The simple level schemes (Figure 10.3) are grossly oversimplified, as the effect of the radiation field has not yet been explicitly considered. We have now to digress, returning to equation (10.1) and consider the eigenstates of H_{rad}, which will be given by zero-photon states $|vac\rangle$ and one-photon states $|\boldsymbol{ke}\rangle$, where $\boldsymbol{k}$ and $\boldsymbol{e}$ label the wave vector and polarisation vector of the photon. For the treatment of linear optical processes, multiphonon states of the radiation field do not have to be included. Additional off-resonance contributions to the decay pattern are negligible.

A possible and convenient choice of the zeroth Hamiltonian is

$$H_0 = H_{M0} + H_{rad} = H - V;\ V = H_V + H_{int} \qquad (10.10)$$

The eigenstates of H_0 consist of zero-photon states $|s,vac\rangle$, $|r,vac\rangle$, $\{|l,vac\rangle\}$, etc. and of one-photon states $|g\ v,\boldsymbol{k}\ \boldsymbol{e}\rangle$. Obviously, the separation of the Hamiltonian as expressed by (10.10) is by no means unique and this can be accomplished in a variety of ways. For example, another useful approach is to adopt the molecular eigenstates (ME) basis $\{|n\rangle\}$, which diagonalises the total molecular Hamiltonian H_M, whereupon

$$H_0 = H_M + H_{rad};\ V = H - H_0 = H_{int} \qquad (10.10a)$$

The eigenstates of H_0 consist now of the one-photon states $|g\ v,\boldsymbol{k}\ \boldsymbol{e}\rangle$ and the zero-photon states $|n,vac\rangle$. The hierarchy of basis sets useful for the description of decay channels in excited molecular states is summarised in Table 10.3.

Realistic level schemes corresponding to the eigenstates of H_0 are displayed in Figure 10.4. The doorway state $|s\rangle$ is simultaneously coupled to the radiation field $\{|g,\boldsymbol{k}\ \boldsymbol{e}\rangle\}$ and to the intramolecular quasi-continuum $\{|l\rangle\}$ in the large molecule or to a sparse vibronic manifold in the small molecule. In the case of the small molecule, two alternative descriptions, which rest on different choices of the zero order Hamiltonian, are illuminating. We may proceed as before, choosing $H_0 = H_{BO} + H_{rad}$, whereupon

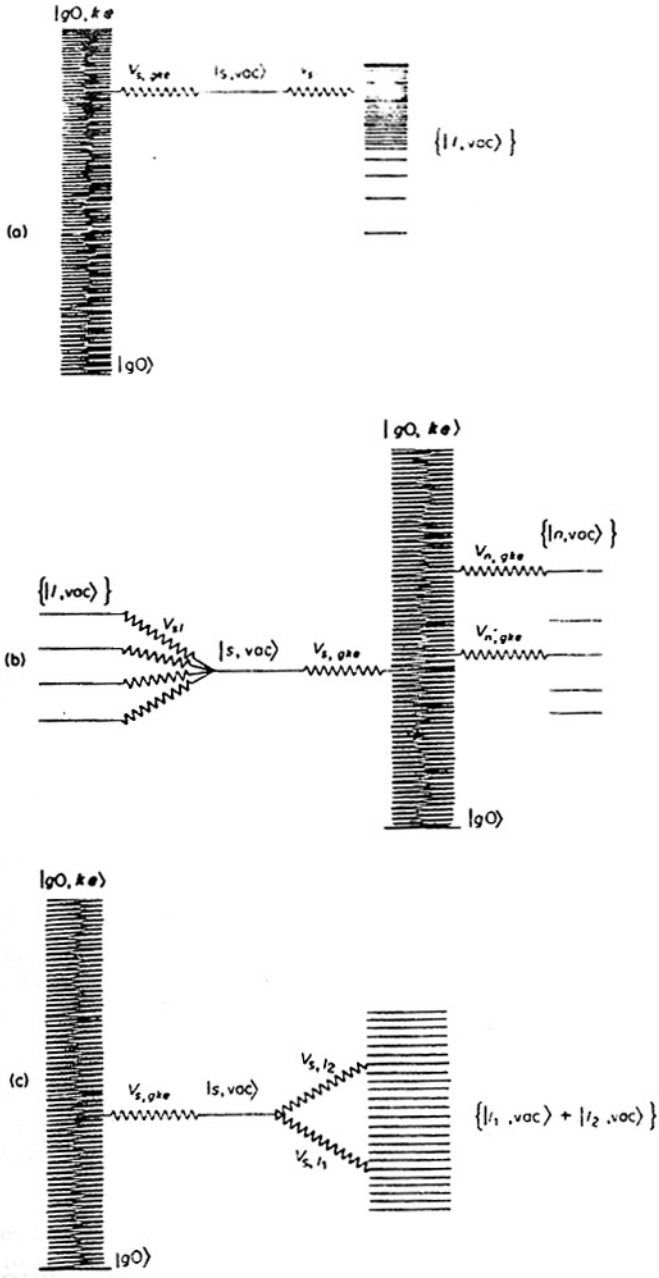

Figure 10.4 Radiative and intramolecular coupling schemes. (a) Radiative and interstate coupling in a large statistical molecule. (b) Radiative coupling in a small molecule. (c) Intermediate level structure in a large molecule

Table 10.3 Basis sets for the description of interstate coupling and electronic relaxation in polyatomics

Basis set	*Major properties*	*Applicability*
Crude-adiabatic basis	a. Diagonalises $H_0^{(CA)}$ b. Comparable near-resonance and off-resonance interactions c. Poor description of potential surfaces	
Born–Oppenheimer basis	a. Diagonalises $H_{MO} - H_{BO}$ b. Off-resonance interactions with higher excited states are negligible	Description of the statistical limit
$\|n,\text{vac}\rangle$	Diagonalises H_M	Radiative decay of small molecules and intermediate-type states of large molecules
$\|j,\text{vac}\rangle$	a. Radiative decay provides the only dissipative channel b. Defined in $\hat{P}$ subspace c. Diagonalises H_{eff} d. Non-orthogonal e. Specifies independently decaying levels	Time evolution of discrete electronically excited states
$\|J,\text{vac}\rangle$	a. System characterised by two parallel decay channels, radiative and non-radiative b–e. As for $\|j,\text{vac}\rangle$ basis	Parallel radiative and non-radiative decay of excited states
$\|\chi\rangle$	Diagonalises H (with zero- and one-photon states)	Proofs of general theorems for the properties of the decay amplitudes

the BO doorway state $|s,\text{vac}\rangle$ is coupled to a sparse manifold $\{|l,\text{vac}\rangle\}$ and to the radiation field. Alternatively, one may look for the molecular eigenstates $\{|n\rangle\}$ which diagonalise the electronic Hamiltonian H_M. The zero-order states of $H_0 = H_M + H_{rad}$ correspond to $|n,\text{vac}\rangle$ which are coupled to the one photon states. If the spacing between the molecular eigenstates considerably exceeds their radiative widths, each of these $|n\rangle$ levels decays (and is excited) independently[71,114]. We thus encounter a situation occurring in atomic physics where, excluding cases of accidental degeneracy, a manifold of well-separated levels (corresponding to the molecular eigenstates) is coupled to the radiation field.

10.4 EXCITATION OF MOLECULAR STATES BY A PHOTON WAVE PACKET

We now proceed to provide a physically realistic description of an optical excitation process. It has been common in many fields, such as atomic and molecular line broadening theory[115] and laser theory[116], to adopt a classical

description of the electromagnetic field, which is ample for the characterisation of the optical excitation process. We shall utilise a quantum mechanical picture for the electromagnetic field, which enables us to consider with ease a time-independent interaction. In this formalism we may take into account the detailed features of the photon statistics of the incident and emitted radiation without confining ourselves to classical fields. The most natural way to excite the molecule is to switch on a photon wave packet at $t = 0$ and follow the subsequent time evolution of the system[76]. It is important to notice that in this experiment we have not necessarily 'prepared' the system in an initial, metastable, decaying state, but rather that this approach is general and can be utilised to describe both limits of 'short excitation' and 'long excitation' experiments. We shall now handle separately the description of the time profile of the photon wave packet and the characteristic molecular decay function, and subsequently show how these two ingredients determine the experimental observables.

Consider first some properties of the photon wave packet, when the molecular system is now absent, so that $H = H_{rad}$. Weak light pulses can be described in terms of a wave packet of one-photon states[71,76]:

$$\Psi_p = \sum_{\boldsymbol{k}} A_{\boldsymbol{k}} |\boldsymbol{k}\, \boldsymbol{e}\rangle = \int \frac{\mathrm{d}^3\boldsymbol{k}}{\sqrt{k}} A_{\boldsymbol{k}} |\boldsymbol{k}\, \boldsymbol{e}\rangle \tag{10.11}$$

where $\boldsymbol{k}$ is the photon wave vector, k corresponds to the photon energy and $|\boldsymbol{k}\rangle$ labels the one-photon state subjected to the normalisation condition $\langle \boldsymbol{k}|\boldsymbol{k}'\rangle = k\delta(\boldsymbol{k} - \boldsymbol{k}')$; $\boldsymbol{e}$ is the photon polarisation direction. The photon density per unit volume at time t is given by[117,118]

$$\rho(x,y,z,t) = [1/(2\pi)^3]|\phi(Q)|^2 \tag{10.12}$$

where

$$\phi(Q) = \int \mathrm{d}^3\boldsymbol{k} \exp(-\mathrm{i}K\cdot Q) A_{\boldsymbol{k}} \tag{10.13}$$

$K = (k,k_x,k_y,k_z)$, and $Q = (ct, x,y,z)$ represent the energy–momentum and the time–space four vectors, respectively. For a light pulse travelling along the x axis, equations (10.11) and (10.13) take the simple form

$$\Psi_p = \sum_{\boldsymbol{k}} A_{\boldsymbol{k}} |\boldsymbol{k}\, \boldsymbol{e}\rangle = \int \frac{\mathrm{d}k}{\sqrt{k}} A_{\boldsymbol{k}} |\boldsymbol{k}\, \boldsymbol{e}\rangle \tag{10.14}$$

$$\rho(x,t) = (1/2\pi)\,|\phi(x + ct)|^2 \tag{10.15}$$

$$\phi(Q) = \phi(x + ct) = \int \mathrm{d}k\, A_k \exp[-\mathrm{i}k(x + ct)] \tag{10.16}$$

Thus the four vector Q reduces to a scalar, while $(1/2\pi)|\phi(x + ct)|^2$ corresponds to the time-dependent spatial profile of the pulse. Let us now define the Fourier transform of the wave packet amplitudes

$$\begin{aligned} \phi(t) &= \int \mathrm{d}k A_k \exp(-\mathrm{i}kt) \\ A_k &= \frac{1}{2\pi} \int \mathrm{d}t\, \phi(t) \exp(\mathrm{i}kt) \end{aligned} \tag{10.17}$$

From equations (10.15) and (10.16) we conclude that $\phi(t) = \phi(x = 0, t)$ whereupon $(2\pi)^{-1/2}\phi(t)$ provides us with the photon density at $x = 0$. It is proper to refer to $\phi(t)$ as the field amplitude. The light pulse can be characterised by its amplitudes $\{A_k\}$, or, alternatively, by the field amplitude function. The general features of the light pulse can be further described by two types of parameters: (i) the energy parameter, $\bar{k}$, defining its mean energy, and (ii) characteristic times which specify the pulse duration and its characteristic rise and fall times.

We shall now present specific examples of photon wave packets which will be subsequently utilised in the study of molecular excitation processes. Consider a wave packet whose amplitudes are given in terms of a coherent, Lorentzian distribution

$$A_k = \frac{(1/2\pi)}{(k - \bar{k} + i\gamma_p/2)} \tag{10.18}$$

where $\bar{k}$ is the centre of the distribution and γ_p its width. The field amplitude for the Lorentzian wave packet is

$$\phi(t) = \begin{cases} 0 & t < 0 \\ \exp(-i\bar{k}t)\exp[-(\gamma_p/2)t] & t > 0 \end{cases} \tag{10.19}$$

As a second example we consider a square pulse of the form:

$$\phi(t) = \begin{cases} \exp(-i\bar{k}t) & 0 < t < T \\ 0 & t < 0,\ t > T \end{cases} \tag{10.20}$$

whose energy profile is

$$A_k = \frac{1}{2\pi}\,\frac{\exp[i(k - \bar{k})T] - 1}{i(k - \bar{k})} \tag{10.21}$$

It is useful at this stage to consider two limiting situations for the pulse amplitudes: (*a*) An ideal 'long time' excitation experiment is characterised by a narrow wave packet $A_k = \delta(k - \bar{k})$ and consequently $|\phi(t)| = 1$. In this case the photon wave packet is well defined in energy. (*b*) When 'short time' excitation conditions are considered we require that $\phi(t) = \delta(t)$ and consequently $A_k = 1/2\pi$. These definitions are general and do not depend on the specific form of $\{A_k\}$.

We now consider excitation and decay processes in a system consisting of an 'isolated' single molecule and the radiation field. At time $t = 0$ the photon wave packet is introduced so that the initial state of the system is a superposition of one-photon states:

$$\psi(0) = \sum_k A_k |g, k\ e\rangle \tag{10.22}$$

This corresponds to a non-stationary state of the Hamiltonian, H, equation (10.1), and exhibits time evolution. As we have chosen H in a time-independent representation, the evolution operator is simply

$$U(t,0) = \exp(-iHt) \tag{10.23}$$

Thus the state of the system at time t is just

$$\psi(t) = \exp(-iHt)\Psi(0) \tag{10.24}$$

$\psi(t)$ can be expanded in terms of a complete set of eigenstates of a zero order Hamiltonian which consists of one-photon states, involving a single ground molecular state $\{|g,k\,e\rangle\}$, and zero-photon excited molecular states $\{|m,\mathrm{vac}\rangle\}$. In the BO representation $|s,\mathrm{vac}\rangle$ and $\{|l,\mathrm{vac}\rangle\} \equiv \{|m,\mathrm{vac}\rangle\}$, while in the ME representation $\{|n,\mathrm{vac}\rangle\} \equiv \{|m,\mathrm{vac}\rangle\}$. Making use of equation (10.22), equation (10.24) can be recast in the general form

$$\psi(t) = \sum_m \sum_k |m,\mathrm{vac}\rangle A_k C_{m,gk\epsilon}(t) + \sum_{k'\epsilon'} \sum_k |gk'\epsilon'\rangle A_k C_{gk'\epsilon',gk\epsilon}(t) \tag{10.25}$$

The time-dependent amplitudes $C_{\alpha\beta}(t)$ with $\alpha,\beta \equiv |m,\mathrm{vac}\rangle$ or $|g,k\,\epsilon\rangle$ are given by

$$C_{\alpha,\beta}(t) = \langle\alpha|\exp(-iHt)|\beta\rangle \tag{10.26}$$

The time-dependent matrix elements of the time evolution operator between the (zero order) eigenstates of H_0 are referred to as the decay amplitudes of the system. These incorporate all the information regarding the molecular decay channels.

Turning now to experimental observables, we can project from (10.25) either the one-photon $\{|g,k'\epsilon'\rangle\}$ states or the vacuum states $\{|m,\mathrm{vac}\rangle\}$. Thus, the probability of finding the system in any excited state at time t is

$$P_e(t) = \sum_m |\langle m,\mathrm{vac}|\psi(t)\rangle|^2 = \sum_m \Big|\sum_k C_{m,gk\epsilon}(t)A_k\Big|^2 \tag{10.27a}$$

while the probability of any one-photon ground electronic state is

$$P_g(t) = \sum_{k'\epsilon'} |\langle g,k'\epsilon'|\psi(t)\rangle|^2 = \sum_{k'\epsilon'} \Big|\sum_{k'} C_{gk'\epsilon',gk'\epsilon'}(t)A_{k'}\Big|^2 \tag{10.27b}$$

The normalisation condition for $\psi(t)$ implies the conservation law

$$P_e(t) + P_g(t) = 1 \tag{10.28}$$

for all t. The total photon counting rate, which monitors the number of photons emitted per unit time, is just $\dot{P}_g(t) = \mathrm{d}P_g/\mathrm{d}t$, which by equation (10.28) is given by $\dot{P}_g(t) = -\dot{P}_e(t)$. We notice that $\dot{P}_g(t)$ counts all photons, including those in the exciting pulse. The experimentally relevant photon counting rate $I(t)$ for all the outcoming photons, excluding those corresponding to the original pulse, is obtained from (10.28) by performing the summation over $k' \neq k$, where k correspond to photon momenta of the pulse:

$$I(t) = \frac{\mathrm{d}}{\mathrm{d}t}\Big(\sum_{k'\epsilon' \neq k\epsilon} |\langle g,k'\epsilon'|\psi(t)\rangle|^2\Big) = \frac{\mathrm{d}}{\mathrm{d}t}\Big(\sum_{k'\epsilon' \neq k\epsilon} \Big|\sum_{k\epsilon} C_{gk'\epsilon',gk\epsilon}(t)A_k\Big|^2\Big) \tag{10.29}$$

For the case of a single optically active state $|s\rangle$,

$$I(t) = \Gamma_s^{\mathrm{r}}|\langle s,\mathrm{vac}|\psi(t)\rangle|^2 \tag{10.30a}$$

where $\Gamma_i^r = 2\pi|\langle \psi_{vac,i}|$ $|^2 \rho_r$ is the radiative width of the $|i\rangle$ state and ρ_r is the density of states in the photon field.

In the general case (see Section 10.6),

$$I(t) = \Gamma_N^r |\langle N,\text{vac}|\psi(t)\rangle|^2 \tag{10.30b}$$

where Γ_N^r is the radiative width of the doorway state $|N\rangle$.

The time evolution of the system can be completely specified by a superposition of products of the pulse amplitudes and of the molecular decay amplitudes, providing a mental, formal separation of the initial conditions of the system (expressed in terms of the $\{A\}$ amplitudes) from the molecular radiative and non-radiative decay processes (expressed via the $\{C\}$ type amplitudes). Whether one can consider excitation followed by a subsequent decay, or alternatively a single-quantum photon scattering process, depends on the specific experimental conditions. We can now proceed to consider separately the amplitudes of the photon wave packet, already discussed in Section 10.3, and the molecular decay amplitudes. The former determine the nature of the excitation process, while the latter are invariant with respect to the nature of the optical excitation.

10.5 MOLECULAR DECAY AMPLITUDES

We now require explicit expressions for the decay amplitudes which are amenable to numerical calculation. It is convenient and practical to introduce at the present stage the Green operator[76, 114]

$$G(E) = (E - H + i\eta)^{-1}; \eta \to 0^+ \tag{10.31}$$

All integrations over (10.31) will be performed over a contour which runs from $-\infty$ to ∞ just above the real E axis. Let us consider at this point the complete set of eigenfunctions $|\chi\rangle$ of the total Hamiltonian H, which satisfy the eigenvalue equation $H\chi = E_\chi\chi$. One can write down immediately the time evolution operator equation and the Green operator in terms of the spectral representation of H,

$$\exp(-iHt) = \sum_\chi |\chi\rangle \exp(-iE_\chi t)\langle\chi| \tag{10.32}$$

and

$$G(E) = \sum_\chi \frac{|\chi\rangle\langle\chi|}{E - E_\chi + i\eta} \tag{10.33}$$

These expressions are not valid for any arbitrary basis, but just for the special basis set $|\chi\rangle$. One can formally recast the time evolution operator in terms of the Fourier transform of the Green function[75, 76]

$$\exp(-iHt) = \frac{1}{2\pi i}\int_{-\infty}^{\infty} \exp(-iEt)G(E)\,dE;\ t > 0 \tag{10.34}$$

where the conventional methods of residue integration have been utilised. Finally, using the formal representation (10.34), the decay amplitudes are explicitly expressed in the form

$$C_{\alpha\beta}(t) \quad (2\pi i)^{-1} \int_{c} \exp(-iEt) G_{\alpha\beta}(E) dE \tag{10.35}$$

involving the matrix elements of the Green function between the zero order states. Thus the evaluation of the decay amplitudes reduces to the calculation of the matrix elements of the Green function.

These general expressions for the decay amplitudes have many attractive features. From the physical point of view, such a general approach is most useful as we are dealing with a large number of molecular levels. From the point of view of mathematical convenience these expressions are quite easy to evaluate. In particular it is a simple matter to relate the matrix elements of $G(E)$ to those of the corresponding Green function for the 'unperturbed' zero order system $G^0(E) = (E - H_0 + i\eta)^{-1}$, where $H_0 \quad H - V$, via the Dyson operator identity[75]. Some more formal and powerful techniques for the evaluation of the relevant matrix elements of the Green function are available[76, 114]. We note that these matrix elements $G_{\alpha\beta}(E)$ are of three types: (i) $\langle g,ke|G(E)|m,\text{vac}\rangle$, (ii) $\langle m,\text{vac}|G(E)|m',\text{vac}$ and (iii) $\langle g,ke|G(E)|g,k'e'\rangle$. The Hilbert space will be partitioned as follows:

$$\hat{P} = \sum_{m} |m,\text{vac}\rangle\langle m,\text{vac}|$$

$$\hat{Q} = \sum_{ke} |g,k\,e\rangle\langle g,k\,e| \tag{10.36}$$

where the subspace $\hat{P}$ contains the excited zero photon levels while the subspace $\hat{Q}$ contains the one-photon zero order states. Provided that we disregard the contribution of the zero-photon ground state and multiphoton excited states, which yield only off-resonance terms, the completeness condition requires that

$$\hat{P} + \hat{Q} = 1 \tag{10.37}$$

We immediately notice that the matrix elements of type (i) combine the $\hat{Q}$ subspace with the $\hat{P}$ subspace, while the matrix elements of type (ii) combine the $\hat{P}$ subspace with itself.

Thus, in view of the orthogonality of the subspaces $\hat{P}$ and $\hat{Q}$, the evaluation of matrix elements of types (i), (ii) and (iii) requires the operators $\hat{Q}G\hat{P}$, $\hat{P}G\hat{P}$ and $\hat{Q}G\hat{Q}$, respectively. The explicit forms for these operators are[76, 114]

$$\begin{aligned}
\hat{Q}G(E)\hat{P} &= (E - \hat{Q}H_0\hat{Q} + i\eta)^{-1}\hat{Q}R(E)\hat{P}(E - H_0 - \hat{P}R(E)\hat{P})^{-1} \\
\hat{P}G(E)\hat{P} &= (E - \hat{P}H_0\hat{P} - \hat{P}R(E)\hat{P})^{-1}\hat{P} \\
\hat{Q}G(E)\hat{Q} &= \hat{Q}(E - \hat{Q}H\hat{Q} + i\eta)^{-1} \\
&\quad + \hat{Q}(E - \hat{Q}H\hat{Q} + i\eta)^{-1}V\hat{P}G(E)\hat{P}V \\
&\quad \times (E - \hat{Q}H\hat{Q} + i\eta)^{-1}\hat{Q}
\end{aligned} \tag{10.38}$$

being expressed in terms of the level shift operator

$$R(E) = V + V\hat{Q}(E - \hat{Q}H\hat{Q})^{-1}\hat{Q}V \tag{10.39}$$

which consists of two contributions: a direct coupling, V, and a relaxation contribution.

To conclude this exposition of the mathematical methods, we would like to point out that the partitioning (10.36) is again not unique, as it is common for many intermediate steps in the formal theory. For some specific systems it is convenient (see Section 10.10) to adopt an alternative partitioning procedure, retaining in the subspace $\hat{P}$ just the discrete excited molecular states and throwing into the subspace $\hat{Q}$ both the radiative continuum and the molecular (zero-photon) continuum (or quasi-continuum) channels.

It is useful to consider the physical implications of these formal results. The poles $E - E_\chi$ are located on the real E axis; thus the system in an eigenstate of H is characterised by a real energy and does not exhibit a decay process. When we consider the matrix element of $G(E)$ between the eigenstates of H_0 the poles of $G(E)$ have imaginary parts of the form $E_s - i/2\Gamma_s$. The imaginary components Γ_s provide the decay rate of a non-stationary state.

10.6 DOORWAY STATES

We shall now derive explicit theoretical expressions for the experimental photon counting rate $I(t)$, equation (10.29), utilising the formal results for the molecular decay amplitudes. Consider the general case of an arbitrary number of excited states which carry oscillator strength from the ground state, whereupon $\langle m,\mathrm{vac}|H_{\mathrm{int}}|g,k\,e\rangle \neq 0$ for several $|m\rangle$ states. Adopting the partitioning of the Hilbert space expressed by (10.36) together with (10.25), (10.36), (10.35) and (10.38) results in

$$I(t) = \frac{\mathrm{d}}{\mathrm{d}t} \sum_{k'e' \neq ke} \left| \frac{1}{2\pi \mathrm{i}} \int_{-\infty}^{\infty} \mathrm{d}E \exp(-\mathrm{i}Et) \times \sum_{ke} \langle g,k'e'|\hat{Q}G(E)\hat{Q}|g,ke\rangle A_k \right|^2 \tag{10.40}$$

Equation (10.38) together with the relation $\hat{Q}V\hat{Q} = 0$ now yield for the matrix element of $\hat{Q}G(E)\hat{Q}$ in equation (10.40),

$$\langle g,k'e'|\hat{Q}G(E)\hat{Q}|g,ke\rangle = \frac{\delta(k - k')|(\delta e,e')}{E - k + \mathrm{i}\eta}$$
$$+ (E - k' + \mathrm{i}\eta)^{-1}\langle g,k'e'|\hat{Q}V\hat{P}G(E)\hat{P}V\hat{Q}|g,ke\rangle(E - k + \mathrm{i}\eta)^{-1} \tag{10.41}$$

The first term on the r.h.s. of (10.41) does not contribute to the sum $k' \neq k$ in (10.29). To pursue further this formal treatment we shall attempt to express the matrix element on the r.h.s. of (10.41) in terms of a generalised doorway state,

$$|N,\mathrm{vac}\rangle = \gamma_N^{-1}\hat{P}V\hat{Q}|g,k_0e_0\rangle = \gamma_N^{-1}\sum_m |m,\mathrm{vac}\rangle\langle m,\mathrm{vac}|H_{\mathrm{int}}|g,k_0e_0\rangle \tag{10.42a}$$

$$\gamma_N^2 = \sum_m |\langle g,k_0e_0|H_{\mathrm{int}}|m,\mathrm{vac}\rangle|^2 = \langle g,k_0e_0|H_{\mathrm{int}}{}^2|g,k_0e_0\rangle \tag{10.42b}$$

We note in passing that the definition of the doorway state $|N,\text{vac}\rangle$ is independent of the choice of the particular one-photon state $|k_0 e_0\rangle$. The generalised doorway state is just a superposition of the excited molecular states each weighted by its coupling strength with the electronic ground-state-radiative continuum $\{|g,ke\rangle\}$. The concept of the generalised doorway state was invoked by Nitzan and Jortner[64, 66] using first-order perturbation theory.

To complete this exposition, (10.41) can be now recast in the form

$$\langle g,k'e'|\hat{Q}G(E)\hat{Q}|g,ke\rangle = \gamma_N^2 \frac{G_{NN}(E)}{(E-k'+i\eta)(E-k+i\eta)}; \quad k'e' \neq ke \tag{10.43}$$

where

$$G_{NN}(E) = \langle N,\text{vac}|G(E)|N,\text{vac}\rangle \tag{10.44}$$

Equation (10.40) with (10.44) results in the general expression for the experimental photon counting rate

$$I(t) = \Gamma_N^r P_N(t) \tag{10.45}$$

where

$$\Gamma_N^r = 2\pi\gamma_N^2\rho_r$$

$$P_N(t) = |\langle N|\psi(t)\rangle|^2 = \gamma_N^2\left|\int_0^t \phi(t-\tau)C_{NN}(\tau)\mathrm{d}\tau\right|^2$$

$$C_{NN}(\tau) = \frac{1}{2\pi i}\int_{-\infty}^{\infty} \mathrm{d}E \exp(-iE\tau)G_{NN}(E) \tag{10.46}$$

Γ_N^r is the radiative width of the $|N\rangle$ state.

The apparently simple form of (10.45) should not mislead us, since in general $C_{NN}(\tau)$ constitutes a superposition of molecular decay amplitudes, which combine excited states:

$$C_{NN}(\tau) = \sum_{m,m'} \langle N,\text{vac}|m,\text{vac}\rangle C_{mm'}(\tau)\langle m,\text{vac}|N,\text{vac}\rangle \tag{10.47}$$

Thus all the relevant information concerning the molecular decay channels is incorporated in the amplitudes in $C_{mm'}(\tau)$. It is important to realise at this point that the entire physical information regarding the molecular decay characteristics is contained in the decay amplitudes $C_{mm'}(\tau)$. Thus, changing the optical excitation conditions, utilising different forms of the field amplitude $\phi(t)$, results in different observed decay-time-resolved photon counting patterns. However, the basic molecular information extracted from such experiments is independent of $\phi(t)$. To provide a physically transparent demonstration let us consider the special case of a single doorway state $|s,\text{vac}\rangle$, whereupon the r.h.s. of (10.47) contains a single term

$$I(t) = \Gamma_s^r|V_{gke,s}|^2\left|\int_{-\infty}^{t} \phi(t-\tau)C_{ss}(\tau)\mathrm{d}\tau\right|^2 \tag{10.48}$$

For the simplest case of photon scattering from a single molecular resonance, the decay amplitude is given by the well known relation

$$C_{ss}(\tau) = \exp(-iE_s\tau)\exp(-\Gamma_s^r\tau/2) \tag{10.49}$$

where E_s is the energy of the zero order state $|s\rangle$ while Γ_s^r corresponds to its radiative decay width, or reciprocal lifetime. We have calculated the experimental photon counting rate resulting from excitation of this system by a light pulse centred at energy $\bar{k}$, whose time profile consists of a constant portion for $0 \leq t \leq T$ followed by an exponential decay characterised by $\tau_p = \gamma_p^{-1}$.[119] The variations of the decay characteristics with changing the off-resonance energy $\Delta = \bar{k} - E_s$ are portrayed in Figure 10.5, where the decay pattern was averaged over the Doppler type inhomogeneous broadening. These numerical data demonstrate that for the time domain $t > T$: (1) At resonance, $\Delta = 0$, only the natural decay time is observed. (2) For the off-resonance situation (when $\gamma_p \gg \Gamma_s^r$) two contributions to the decay pattern are exhibited, which are determined by the pulse decay time and by the molecular decay time, respectively. (3) Far off-resonance (when $\Delta \gg \gamma_p \gg \Gamma_s^r$) the ratio of the two decay components (at $t = T$) is constant, of the order $\exp(\Gamma_s^r T)$, independent of Δ. These results demonstrate the continuous transition between time-resolved resonance fluorescence and near-resonance Raman scattering, recently studied by Williams *et al.*[120] from a

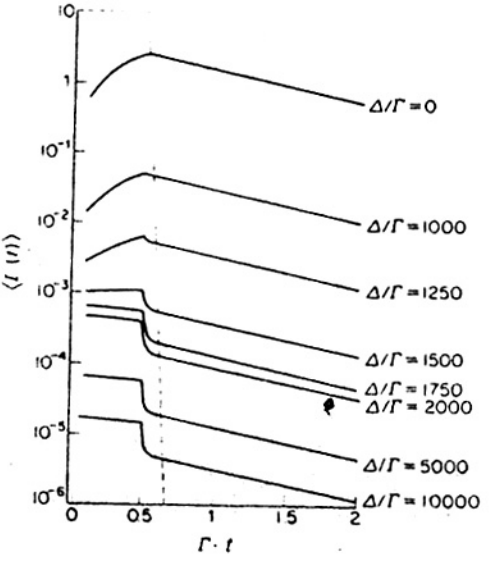

Figure 10.5 Model calculations for time-resolved decay pattern of a single molecular resonance excited by a composite pulse whose time profile is characterised by a constant duration for $0 \leq t \leq T$ followed by an exponential decay with a lifetime γ_p^{-1} (dashed line). The experimentally relevant photon counting rate $I(t)$ is given for various values of the off-resonance energy parameter Δ. The effects of Doppler broadening are specified in terms of a Gaussian distribution with a width β. The following parameters are employed: $\gamma_p/\Gamma_s^r = 100$, $\Gamma_s^r T = 0.5$ and $\beta/\Gamma_s^r = 500$ expressed in terms of the resonance width Γ_s^r

single rovibrational level of the $B^3\Pi$ state of I_2. For the sake of the present discussion we note that the only molecular parameter which can be extracted from experiment is the decay time $(\Gamma_f^r)^{-1}$.

We are now in a position to provide criteria for the applicability of the concept of 'decay of an initially excited state' and its range of validity, and also to specify the general conditions for 'short excitation' and 'long excitation' experiments.

The understanding of the nature of the 'initially prepared' optically excited state is crucial for the understanding of any short excitation decay experiment when one wants to formulate the precise conditions for validity of the separation of the excitation and decay processes. Early treatments of this problem considered the radiative excitation process to lowest order and accounted for the non-radiative decay during the excitation process[30,31,77]. The original treatments were grossly oversimplified as they disregarded the radiative decay channel. Rhodes[79] has utilised the density matrix formalism to follow the time evolution after the termination of the pulse. For long excitation times the density matrix assumes a partially diagonal form[79]; however, this does not affect the decay characteristics in the statistical limit[30,41]. Freed[78] has treated the excitation–decay process by starting from the system at $t = 0$ in the state $|g,ke\rangle$ and subsequently terminating the photon field after an arbitrary time; $\psi(t = 0)$ in his formalism is precisely defined in energy and thus this approach is adequate for long-time excitations rather than for short excitation experiments. The definition of an 'initially excited' state is essentially a theoretical problem, as it does not involve an experimental observable. In order to provide a meaningful definition for this concept two basic conditions have to be satisfied. (i) A single state has to be defined which is radiatively coupled to and carrying all the oscillator strength from the ground state. (ii) The duration of the exciting pulse is appreciably shorter than all the (radiative and non-radiative) 'decay times' (or reciprocal widths) of the excited states. A detailed treatment of the problem in terms of the effective Hamiltonian formalism (see Section 10.7) was recently provided[71].

10.7 EFFECTIVE HAMILTONIAN FORMALISM

Let us introduce and explore an effective Hamiltonian which specifies the time evolution of the excited molecular states in the presence of the radiation field. The use of such effective Hamiltonians is common in fields such as magnetic resonance, where in handling relaxation problems one considers the time evolution of a small part of the system. In our problem we shall consider the time evolution of the subpart $\{|m,\text{vac}\rangle\}$ consisting of all discrete, zero-photon, electronically excited states. Adopting the generalised Wigner–Weisskopf approximation[121], Bixon *et al.*[44] have demonstrated that the time evolution of the discrete excited molecular states in the presence of the radiation field can be described in terms of an effective Hamiltonian. The same argument was provided[33,78] in terms of the Green's function formalism.

The definition of the effective Hamiltonian for the excited states rests on the following observations

(1) The Hilbert space is partitioned into the subspaces $\hat{P}$ and $\hat{Q}$.

(2) The photon counting rate, $I(t)$, equation (10.45), is determined by decay amplitudes combining levels in the $\hat{P}$ subspace.

(3) From (1) and (2) it follows that the evaluation of the relevant decay amplitudes requires the matrix elements of $\hat{P}G\hat{P}$ between excited states.

(4) The operator $\hat{P}G\hat{P}$, equation (10.38), is rewritten in the form

$$\hat{P}G(E)\hat{P} = \hat{P}(E - H_{\text{eff}})^{-1}\hat{P} \tag{10.50}$$

where the effective Hamiltonian in the $\hat{P}$ subspace is

$$H_{\text{eff}} = \hat{P}(H_0 + R)\hat{P} \tag{10.51}$$

(5) The evolution operator in the $\hat{P}$ subspace can be formally represented utilising equation (10.34)

$$\hat{P}U(t,0)\hat{P} = \int_{-\infty}^{\infty} dE \exp(-iEt)\hat{P}G(E)\hat{P} \tag{10.52}$$

Now, making use of (10.50) we obtain

$$\hat{P}U(t,0)\hat{P} = \frac{1}{2\pi i}\int_{-\infty}^{\infty} dE\hat{P}\frac{\exp(-iEt)\hat{P}}{E - H_{\text{eff}}} = \hat{P}\exp(-iH_{\text{eff}}t)\hat{P} \tag{10.53}$$

(6) A set of states $\{|j,\text{vac}\rangle\}$, defined in the $\hat{P}$ subspace, which diagonalise the effective Hamiltonian can be then used for the spectral representation of $\hat{P}G\hat{P}$ and of the evolution operator in the $\hat{P}$ subspace.

To explore the general form of the effective Hamiltonian, equation (10.50), we utilise the definition of the level shift operator, equation (10.39), together with the relations $\hat{P}(H_{\text{rad}} + H_{\text{int}})\hat{P} = 0$ and $\hat{P}V\hat{Q} = \hat{P}H_{\text{int}}\hat{Q}$. The effective Hamiltonian can now be recast in the matrix form

$$H_{\text{eff}} = H_M + \Delta - (i/2)\Gamma \tag{10.54}$$

where it is understood that H_{eff} combines only $|m,\text{vac}\rangle$ states in the $\hat{P}$ subspace. The explicit forms for the level shift matrix Δ, and for the decay matrix Γ are obtained from the relaxation contribution of the level shift operator, equation (10.39)

$$\Delta(E) = \text{PP}\int \frac{H_{\text{int}}|g,ke\rangle\langle g,ke|H_{\text{int}}}{E - k}\rho_r(k)dk \tag{10.55}$$

$$\Gamma(E) = 2\pi H_{\text{int}}|g,ke\rangle\rho_r(E)\langle g,ke|H_{\text{int}} \tag{10.56}$$

where $\rho_r(E) \equiv \rho_r(k)$ is the density of states in the radiation field; we have set $E_g = 0$ and PP represents the Cauchy principal part of the integral.

The matrix element of the level shift matrix are

$$\Delta_{mm'} = \text{PP}\int \frac{\langle m,\text{vac}|H_{\text{int}}|g,ke\rangle\langle g,ke|H_{\text{int}}|m',\text{vac}\rangle}{E - k}\rho_r(k)dk \tag{10.57}$$

This is a generalisation[114] of the concept of the ordinary level shift of a single resonance (i.e. single level interacting with a continuum). The elements of the (real) level shift matrix (10.55) diverge when the integration over k is performed to infinity, as $\rho_r(k) \propto k^2$. This well known difficulty[117] of quantum electrodynamics is solved by a renormalisation procedure as in the theory of the Lamb shift. The diagonal and off-diagonal matrix elements of Δ are expected to be of the order of[72] $\Delta \approx L''/n$, where $L'' \approx 10^{-2}\,\mathrm{cm}^{-1}$ is the hydrogenic Lamb shift and n is the number of effectively coupled levels. Then Δ varies from $10^{-2}\,\mathrm{cm}^{-1}$ for a small number of coupled levels to $10^{-6}\,\mathrm{cm}^{-1}$ for a dense distribution. These terms will result in radiative shifts of the real part of H_{eff} and they are of minor practical interest. When the coupling between zero order discrete states and an intramolecular continuum is considered (see Sections 10.11 and 10.12), the level shift contribution has to be included when the coupling terms and/or the density of states exhibit a rapid variation with energy. The level shift term may result in the appearance of 'new' states near the continuum threshold[50]. In the case of non-adiabatic coupling between discrete zero order and an intramolecular continuum, $\Delta_{mm} \approx \Gamma_{mm}$ and in some cases of predissociation[96] the level shift contribution is important in modifying the energy levels.

Of central importance is the damping matrix (10.56) which is explicitly given in the form

$$\Gamma_{mm'} = 2\pi\langle m,\mathrm{vac}|H_{\mathrm{int}}|g,ke\rangle\langle g,ke|H_{\mathrm{int}}|m',\mathrm{vac}\rangle\rho_r \qquad (10.58)$$

The following features of the damping matrix should be noted: (*a*) Γ provides a generalisation of the Fermi golden rule. For the decay of a single resonance, the resonance width (or the reciprocal decay time) is given by Γ_{mm}. (*b*) Γ is in general non-diagonal. (*c*) Γ is Hermitian. (*d*) Γ is a slowly varying function of the energy in the range of interest. (*e*) The off-diagonal matrix elements of Γ represent coupling between the $\{|m,\mathrm{vac}\rangle\}$ states via the one-photon states. These off-diagonal contributions are important only in the case of near degeneracy when these terms are comparable with the energy spacing between the energy levels, i.e. $\Gamma_{mm'} \approx |E_m - E_{m'}|$.

We now proceed to explore the general properties of the effective Hamiltonian.

1. The effective Hamiltonian is non-Hermitian. This can be rationalised by noting that we consider only a subspace of the Hilbert space consisting of the (discrete) zero-photon manifold. In fact, from the basic definition (10.54) and from the Hermitian property of Γ we conclude that H_{eff} is in general a sum of a Hermitian matrix H_{M} and an anti-Hermitian matrix $-(\mathrm{i}/2)\,\Gamma$.

2. When the effective Hamiltonian is non-diagonal within a given basis of zero-photon states, say $\{|m,\mathrm{vac}\rangle\}$, these states cannot be considered to decay independently.

3. One can find, in principle, for the general case and in practice for simple model systems, a basis of zero-photon states $\{|j,\mathrm{vac}\rangle\}$ which diagonalises the effective Hamiltonian, via the transformation

$$\begin{pmatrix} |j_1,\mathrm{vac}\rangle \\ |j_2,\mathrm{vac}\rangle \\ \vdots \end{pmatrix} = \boldsymbol{D}\begin{pmatrix} |m_1,\mathrm{vac}\rangle \\ |m_2,\mathrm{vac}\rangle \\ \vdots \end{pmatrix} \qquad (10.59)$$

4. The effective Hamiltonian is diagonalised by the transformation

$$\boldsymbol{D}\,\boldsymbol{H}_{\text{eff}}\boldsymbol{D}^{-1} = \boldsymbol{\Lambda} \tag{10.60}$$

where $\boldsymbol{\Lambda}$ is diagonal, i.e. $\Lambda_{ij} = \Lambda_{ii}\delta_{ij}$.

5. As H_{eff} is a sum of an Hermitian matrix H_M and an anti-Hermitian matrix $-(i/2)\,\boldsymbol{\Gamma}$, $\boldsymbol{D}$ is a non-unitary matrix. When we use a basis set $\{|m\rangle\}$ of real functions, H_{eff} constitutes a complex symmetric matrix and it can be diagonalised using an orthogonal (non-unitary) transformation matrix $\boldsymbol{D}$, i.e. $\boldsymbol{D}^{-1} = \boldsymbol{D}$.

6. The matrix elements of the diagonal matrix $\boldsymbol{\Lambda}$ are in general complex $\Lambda_{jj'} = [E_j - (i/2)\Gamma_j]\delta_{jj'}$.

7. The new basis set $\{|j,\text{vac}\rangle\}$ which diagonalises H_{eff} is characterised by complex energies $E_j - (i/2)\,\Gamma_j$. It is natural to assign the real part $\text{Re}\,\Lambda_{jj}$ to the energies E_j of these states while the imaginary parts $\text{Im}\,\Lambda_{jj} = -(i/2)\Gamma_j$ correspond to characteristic widths of the levels in the presence of the radiation field.

8. The diagonal sum rule applies to the transformation (10.60). Thus

$$\text{Re}[T_r\,\boldsymbol{\Lambda}] = \text{Re}\,T_r\,[H_{\text{eff}}] = T_r\,H_M \tag{10.61}$$

Equation (10.61) implies that $\sum_j E_j = \sum_m E_m$, which is the conventional diagonal sum rule. Furthermore, we have the more interesting result $\sum_j \Gamma_j = \sum_m \Gamma_{mm}$. Thus the sum of the widths of the $\{|j,\text{vac}\rangle\}$ states is equal to the sum of the diagonal elements of the (non-diagonal) $\boldsymbol{\Gamma}$ matrix in any $\{|m,\text{vac}\rangle\}$ representation.

9. The $\{|j,\text{vac}\rangle\}$ basis set is not orthogonal. This is a consequence of the anti-Hermitian property of $(i/2)\boldsymbol{\Gamma}$ which causes the non-unitarity of $\boldsymbol{D}$.

10. In order to expand $\hat{P}$ in terms of diagonalised projections we shall now define the complementary basis set $\{j,\text{vac}\rangle\}$ by the relation:

$$\begin{pmatrix} |j_1,\text{vac}\rangle \\ |j_2,\text{vac}\rangle \\ \vdots \end{pmatrix} = (\boldsymbol{D}^{-1})^{\dagger} \begin{pmatrix} |m_1,\text{vac}\rangle \\ |m_2,\text{vac}\rangle \\ \vdots \end{pmatrix} \tag{10.62}$$

In the special case when the $|m,\text{vac}\rangle$ basis set has a real representation, the wave function corresponding to $|j_x,\text{vac}\rangle$ is the complex conjugate of the wave function for $|j_x,\text{vac}\rangle$. We can thus write for the general case[71] $\hat{P} = \sum_j |j,\text{vac}\rangle\langle j,\text{vac}|$.

11. The time evolution operator (10.53) is

$$\hat{P}U(t,0)\hat{P} = \hat{P}\exp(-iH_{\text{eff}}\,t)\hat{P} = \sum_j |j,\text{vac}\rangle \exp[-i\Lambda_{jj}t]$$
$$\times \langle j,\text{vac}| = \sum_j |j,\text{vac}\rangle \exp[-iE_jt - \tfrac{1}{2}\Gamma_j t]\langle j,\text{vac}| \tag{10.63}$$

This general result implies that the decay amplitudes combining any pair of $|m,\text{vac}\rangle$ states will be expressed as a superposition of terms of the form $\exp[-(\Gamma_j/2)t - iE_jt]$, i.e. a sum of independently decaying exponentials. The basis set $|j,\text{vac}\rangle$ can be considered as the set of *independently decaying levels* characterising the molecular system.

12. Finally, we shall recast the Green's function in the $\hat{P}$ subspace in the spectral representation of the independently decaying levels $|j,\text{vac}\rangle$. Making use of (10.34) and (10.63) we obtain

$$\hat{P}G(E)\hat{P} = \sum_j \frac{|j\rangle\langle j|}{E - E_j + (i/2)\Gamma_j} \tag{10.64}$$

which is, of course, nothing but the inverse Fourier transform of (10.63). This result will be useful for the study (see Section 10.14) of absorption and photon scattering cross sections in a system characterised by a large number of closely spaced levels.

10.8 GENERAL THEORY OF TIME EVOLUTION OF EXCITED STATES

We are now able to provide explicit expressions for the decay amplitudes which describe the time evolution of the excited states. Equation (10.46) with the aid of (10.64) takes the form

$$C_{NN}(\tau) = \sum_j \langle N,\text{vac}|j,\text{vac}\rangle \exp\left[-iE_j\tau - (\Gamma_j/2)\,\tau\right]\langle j,\text{vac}|N,\text{vac}\rangle \tag{10.65}$$

Thus (10.45) is

$$I(t) = \Gamma_N^r\left\{\sum_{jj'} A_j^* A_j F_{j'}^{P*}(t)F_j^P(t) = \sum_j |A_j|^2|F_j^P(t)|^2 + 2\text{Re}\sum_{j'>j} A_{j'}^* A_j F_{j'}^{P*}(t)F_j^P(t)\right\} \tag{10.66}$$

where the coefficients are

$$A_j = \langle N|j\rangle\langle j|N\rangle \tag{10.67}$$

while the time-dependent amplitudes are given by

$$F_j^P(t) = \int_0^t d\tau\, \phi(t-\tau)\exp(-iE_j\tau)\exp\left(-\frac{\Gamma_j}{2}\tau\right) \tag{10.68}$$

The photon counting rate [equation (10.45)] is

$$I(t) = \Gamma_N^r \sum_j \sum_{j'} A_j A_{j'}^* F_{j'}^{P*}(t)F_j^P(t) \tag{10.69}$$

We can also obtain a useful expression for the population probability, $P_e(t)$, of all excited states

$$P_e(t) = \sum_j \sum_{j'} A_{jj'} F_{j'}^P(t)F_j^{P*}(t)$$

$$A_{jj'} = \langle N,\text{vac}|j,\text{vac}\rangle\langle j,\text{vac}|j',\text{vac}\rangle\langle j',\text{vac}|N,\text{vac}\rangle \tag{10.70}$$

To bring (10.66) and (10.69) into a more tractable form let us utilise the Lorentzian photon wave packet [equation (10.18)] for optical excitation. In this special case

$$F_j^p(t) = \frac{\exp[-iE_j t]\exp[-\Gamma_j t/2] - \exp[-i\bar{k}t]\exp[-\gamma_p t/2]}{\bar{k} - E_j + i[(\Gamma_j - \gamma_p)/2]} \tag{10.68a}$$

From these results we can immediately draw some general conclusions for the time evolution of a system of closely spaced levels. (*a*) The time evolution of the excited states is expressed in terms of cross products of the functions $F_j^p(t)$. (*b*) It is important to notice that the matrix $A_{j'j}$, equation (10.70), is not diagonal in view of the non-orthogonality of the basis set $\{|j,\text{vac}\rangle\}$. (*c*) Each of the functions $F_j^p(t)$ incorporates dual information. It contains the molecular energies E_j and widths Γ_j of the independently decaying levels, together with relevant energy parameters $\bar{k}$ and γ_p, which characterise the maximum energy and the width of the exciting pulse. (*d*) The time-independent denominators in F_j^p provide the attentuation factors for absorption of the pulse energy by the $|j,\text{vac}\rangle$ levels. (*e*) In the limit $t \to \infty$, $F_j^p(t) \to 0$ for all j, irrespective of the relation between γ_p and $\{\Gamma_j\}$. This implies that $P_e(\infty) = 0$. Thus for a physical system characterised by a discrete spectrum of excited states the total photon emission yield at $t = \infty$ is unity, i.e. $P_q(\infty) = 1$. It is important to stress that we have considered a discrete molecular spectrum. When the spectrum of H_{BO} (or of H_M) contains continuum states we should not incorporate them in the $\hat{P}$ subspace. Under these more complicated circumstances we have to include the zero-photon continuum molecular states in the $\hat{Q}$ subspace while the $\hat{P}$ subspace contains only discrete levels. Under these conditions the probability that the system is in the (extended) $\hat{Q}$ space at $t = \infty$ is still unity; however, the photon emission yield at $t = \infty$ may be lower than unity owing to the branching between the radiative channels and the non-radiative continuum channels. (*f*) In the limit of high-energy resolution of the exciting pulse, $\gamma_p \ll \Gamma_j$ and the contribution to the $F_j^p(t)$ functions originating from the molecular lifetimes Γ_j is masked by the long decay time of the pulse. Under these circumstances of 'long time excitation' the time-resolved photon counting rate does not yield any relevant information regarding the 'molecular' widths. (*g*) In the limit of a broad excitation pulse we encounter the 'short excitation' experiment and the time-resolved decay pattern is exhibited.

10.9 THEORY OF 'SHORT TIME' EXCITATION EXPERIMENTS

We can now provide a realistic discussion of the 'preparation' of metastable states by requiring that the energetic spread γ_p of the photon wave packet considerably exceeds the characteristic widths Γ_j for all the independently decaying levels, i.e.

$$\gamma_p \gg \Gamma_j \tag{10.71}$$

for all j. Under these circumstances the functions $F_j^p(t)$, equation (10.70), take the form

$$F_j^*(t) = \frac{\exp[-iE_j t]\exp[-(\Gamma_j/2)t]}{E_j - \bar{k} + i\gamma_p/2} \tag{10.72}$$

The time evolution of the excited states resulting from the realistic 'short time' excitation experiment can be now written utilising (10.70) and (10.72):

$$P_e(t) = \sum_j \frac{A_{jj}}{(E_j - \bar{k})^2 + (\gamma_p/2)^2} \exp(-\Gamma_j t)$$
$$+ 2\mathrm{Re} \sum_{j \neq j'} \sum \frac{A_{j'j} \exp[i(E_{j'} - E_j)t - \frac{1}{2}(\Gamma_j + \Gamma_{j'})t]}{[E_j - \bar{k} + i\gamma_p/2][E_{j'} - \bar{k} - i\gamma_p/2]} \tag{10.73}$$

The attenuation factors $(E_j - \bar{k} \pm i\gamma_p/2)$ appearing in the denominator of (10.73) account for the different absorption strength of the exciting pulse by the various independently decaying levels $|j,\mathrm{vac}\rangle$. To treat excitation by a white pulse we introduce a second condition for the pulse width

$$\gamma_p \gg |E_j - \bar{k}| \tag{10.74}$$

for all E_j, which implies that the pulse width exceeds the energy spread of $\{|j,\mathrm{vac}\rangle\}$. When both conditions (10.71) and (10.74) are simultaneously satisfied

$$P_e(t) = (4\Gamma_N^r/\gamma_p^2) \sum_{jj'} A_{j'j} \exp[i(E_{j'} - E_j)t - \tfrac{1}{2}(\Gamma_j + \Gamma_{j'})t] \tag{10.75}$$

corresponding to extremely broad excitation conditions.

Equation (10.71) provides the necessary condition for a realistic broad band excitation. This result is useful for the study of a sparse distribution of strongly coupled levels as in interstate coupling in small molecules[32,33,113]. The combination of conditions (10.71) and (10.74) specifies the circumstances equivalent to a delta function excitation in time, which are useful for the study of systems of closely spaced levels, i.e. a dense level structure in the excited states of large molecules.

The experimental information regarding the decay features originates from the photon counting rate. When only condition (10.71) is satisfied, we obtain from (10.73) for the realistic short-time excitation experiment:

$$I(t) = \Gamma_N^r \{ \sum_j \frac{|A_j|^2 \exp(-\Gamma_j t)}{(E_j - \bar{k})^2 + (\gamma_p/2)^2}$$
$$+ \sum_{j \neq j'} \frac{A_{j'}^* A_j}{[E_j - \bar{k} + (i/2)\gamma_p][E_{j'} - \bar{k} - (i/2)\gamma_p]} \times$$
$$\exp[i(E_{j'} - E_j)t] \exp[-\tfrac{1}{2}(\Gamma_j + \Gamma_{j'})t] \} \tag{10.76}$$

Now, for a system of densely spaced excited levels, we can invoke the additional condition (10.74) whereupon (10.76) is simplified to

$$I(t) = (4\Gamma_N^r/\gamma_p^2) \sum_{jj'} A_{j'}^* A_j \exp\left[-\frac{\Gamma_j + \Gamma_{j'}}{2} + i(E_{j'} - E_j)\right] \tag{10.77}$$

From these results we conclude that the radiative decay of a system of discrete excited levels exhibits the following features. (*a*) The photon counting rate can in general be recast in terms of a linear superposition of a sum of direct exponentials and of a sum of oscillatory terms. (*b*) The feasibility of observing the oscillatory pattern of the decay originating from the cross terms is crucially determined by the nature of the physical system. (*c*) When the spacings between the $|j\rangle$ levels considerably exceed their radiative widths, i.e. $\Gamma_j, \Gamma_{j'} \ll |E_j - E_{j'}|$ for all j and j', the oscillatory terms exhibit extremely fast oscillations on the timescale Γ_j^{-1} or $\Gamma_{j'}^{-1}$. For a system of coarsely spaced j levels, no oscillatory contributions to the decay should be experimentally observed and the radiative decay rate is determined by a linear superposition of decaying exponentials. (*d*) For the opposite extreme case of a dense level distribution with a single (zero order) $|s\rangle$ level acting as a doorway state, there is a large number of cross terms in (10.76) or (10.77). These oscillatory terms lead to a destructive interference effect resulting in shortening of the radiative decay time on the experimentally relevant timescale in a large statistical molecule (see Section 10.12). (*e*) Interference effects, i.e. quantum beats, in the radiative decay of an isolated molecule can be experimentally observed only for a system characterised by a small number of closely spaced $|j,\text{vac}\rangle$ levels where $\Gamma_j, \Gamma_{j'} \approx |E_j - E_{j'}|$. This situation requires effective coupling between a small number of zero order molecular levels corresponding to two electronic configurations. In real life it may be possible[51] to observe quantum beats in the decay of an excited state of a large molecule which corresponds to the intermediate level structure. (*f*) From the point of view of general methodology it is important to notice that the oscillatory terms which may result in observable quantum beats are exhibited both in the probability for population of the excited state, $P_e(t)$, and of the ground state, $P_g(t)$. Thus the phenomenon of quantum beats in the radiative decay rate originates from the ocillations of the system between its electronically excited zero-photon level. 'Recurrence oscillations'[122] in the excited state cannot be distinguished from quantum beats in the radiative decay.

To conclude this discussion let us consider the nature of an 'initially prepared' metastable decaying state for a complex level structure. In the case of an ultra-short excitation pulse, the answer is obvious as $\psi(0) = |N,\text{vac}\rangle$ and the general doorway state constitutes the 'initially prepared' state. Under general and more realistic excitation conditions, e.g. for a square-pulse excitation, equation (10.20), we can define the excited state at $t = T$ by the projection $\hat{P}\psi(t)$, which can be expressed as a superposition of the independently decaying levels:

$$\hat{P}\psi(T) = \sum a_j(T)|j,\text{vac}\rangle \tag{10.78}$$

where the expansion coefficients are

$$a_j(T) = \langle j,\text{vac}|N,\text{vac}\rangle F_j^p(T) \tag{10.79}$$

This result can be utilised to define the nature of the metastable state at any instant of a 'short excitation' experiment. Apart from the simple case

of a single resonance, the nature of the metastable state, [equation (10.78)], is determined by the excitation conditions.

10.10 PARALLEL DECAY

We have provided a general recipe for handling the problem of the radiative decay of a manifold of discrete levels. In this case, $P_e(t = \infty) = 0$ and $P_g(t = \infty) = 1$, so that no discrete levels are populated in the distant future and $Y(\infty) = 1$. We can encounter a situation when $Y(\infty) < 1$ provided that the excited molecular states contain a molecular continuum (or a dense quasi-continuum) $\{|lc,\text{vac}\rangle\}$ characterised by the density of states ρ_e, e.g. a dissociative intramolecular continuum in the case of predissociation or an intramolecular quasi-continuum in the case of electronic relaxation in the statistical limit. Consider now the simplest common situation where the radiative continuum $|g,ke\rangle$ and the molecular zero-photon continuum $|lc,\text{vac}\rangle$ are not directly coupled, i.e. $\langle g,ke|V|lc,\text{vac}\rangle = 0$; we partition the Hilbert space by incorporating in the $\hat{P}$ subspace the discrete zero photon excited states, as before

$$\hat{P} = \sum_m |m,\text{vac}\rangle\langle m,\text{vac}| \tag{10.80}$$

while the $\hat{Q}$ subspace contains the two continua, that is

$$\hat{Q} = \hat{Q}_r + \hat{Q}_l \tag{10.81}$$

$$\hat{Q}_r = \sum_{ke} |g,ke\rangle\langle g,ke|$$

$$\hat{Q}_l = \sum_{lc} |lc,\text{vac}\rangle\langle lc,\text{vac}| \tag{10.82}$$

For most practical purposes we can consider the decay amplitudes which combine only the (discrete) states in the $\hat{P}$ subspace. One can then extend the definition of the effective Hamiltonian[71] to handle the situation of a discrete manifold $\{|m,\text{vac}\rangle\}$ simultaneously coupled to two continua. The generalised effective Hamiltonian is

$$H_{\text{eff}} = \hat{P}[H_M + \Delta - (i/2)\,\gamma]\hat{P} \tag{10.83}$$

where Δ and γ are generalised level shift and decay matrices, respectively, now given in the explicit form

$$\Delta_{mm'} = \text{PP}\int dk\, \frac{\langle m,\text{vac}|H_{\text{int}}|g,ke\rangle\langle g,ke|H_{\text{int}}|m',\text{vac}\rangle}{E - E_l}\rho_r(k)$$

$$+ \text{PP}\int dE_l\, \frac{\langle m,\text{vac}|H_V|lc,\text{vac}\rangle\langle lc,\text{vac}|H_V|m',\text{vac}\rangle}{E - E_l}\rho_l(E_l) \tag{10.84}$$

and

$$\gamma_{mm'} = 2\pi\langle m,\text{vac}|H_{\text{int}}|g,ke\rangle\langle g,ke|H_{\text{int}}|m,\text{vac}\rangle\rho_r$$

$$+ 2\pi\langle m,\text{vac}|H_V|lc,\text{vac}\rangle\langle lc,\text{vac}|H_V|m',\text{vac}\rangle\rho_l \tag{10.85}$$

We can proceed as in Section 10.7 to find the basis set $|J,\mathrm{vac}\rangle$ which diagonalises the effective Hamiltonian (10.83): $(H_{\mathrm{eff}})_{JJ} = (E_J - (i/2)\gamma_J)\delta_{JJ'}$, while for the complementary basis set $|\bar{J},\mathrm{vac}\rangle$ we have $(H_{\mathrm{eff}})_{\bar{J}\bar{J}'} = (E_{\bar{J}} - (i/2)\gamma_{\bar{J}})\delta_{\bar{J}\bar{J}'}$. The decay widths of the independently decaying levels $|J,\mathrm{vac}\rangle$ contain both radiative and non-radiative contributions. Finally, the evolution operator in the $\hat{P}$ subspace is,

$$\hat{P}U(t,0)\hat{P} = \sum_J |J,\mathrm{vac}\rangle \exp[-iE_J t - (1/2)\gamma_J t]\langle J,\mathrm{vac}| \qquad (10.86)$$

It is a simple matter to extend the formalism presented in Sections 10.8 and 10.9 to include the role of the additional intramolecular decay channel. To obtain the time evolution of the discrete states one has just to replace E_J by E_J and the radiative widths Γ_J by the total widths γ_J in equations (10.68)–(10.70) for the general excitation and in equations (10.73)–(10.77) for the 'short time' excitation. It is important to realise that $P_e(t)$ represents the time-dependent population of the excited discrete states and not of all excited states, so that $P_g(t) + P_e(t) = P_e(t)$ and $\dot{P}_g(t) = -\dot{P}_e(t) = -\dot{P}_e(t)$ where $P_c(t)$ is the occupation probability of the $\{|I_c\rangle\}$ intramolecular continuum. To gain some insight into the nature of the modifications introduced by the presence of additional intramolecular decay channels, let us write the photon counting rate for the excitation which satisfies both conditions (10.71) and (10.74),

$$I(t) = \Gamma_N^r \sum_J \sum_{J'} B_J B_{J'}^* \exp[-i(E_J - E_{J'})t] \exp[-\tfrac{1}{2}(\gamma_J + \gamma_{J'})t] \qquad (10.87)$$

where

$$B_J = \langle N|J\rangle\langle J|N\rangle \qquad (10.88)$$

From these results we conclude that for the simplest case of parallel radiative and non-radiative decay: (*a*) The time-dependent decay pattern is determined by the total widths γ_J of the independently decaying states. When the effective Hamiltonian is non-diagonal these total widths have to be obtained from the general procedure outlined herein. (*b*) Interference effects in the time evolution and in the photon counting rate of a system consisting of a small number of discretely coupled zero order excited states undergoing parallel decay may be exhibited. Quantum beats will be observed provided that the spacings between the small number of $|J,\mathrm{vac}\rangle$ levels are comparable with their total widths, i.e. γ_J and $\gamma_{J'} \sim |E_J - E_{J'}|$ for all J and J'. Quantum beats will not be observed for a dense manifold of a large number of levels and for a manifold of extremely broadened levels where γ_J and $\gamma_{J'} \gg |E_J - E_{J'}|$ (*c*) For a system of a small number of levels undergoing paralled decay it may be possible to vary continuously the γ_J widths via external perturbations and consequently modify the decay into the non-radiative relaxation channel. Then interference effects may be exhibited for a narrow range of γ_J values. No experimental evidence for this effect is yet available.

Consider the simplest situation where a single level $|s,\mathrm{vac}\rangle$ exhibits parallel decay into radiative and non-radiative continua. Now $\hat{P} = |s,\mathrm{vac}\rangle\langle s,\mathrm{vac}|$ while $\hat{Q}$ is given by equation (10.82). There is a single state in the $|J,\mathrm{vac}\rangle$ manifold, i.e. $|J,\mathrm{vac}\rangle \equiv |s,\mathrm{vac}\rangle$. The time evolution of the excited state under

the general conditions of wave packet excitation is obtained from equation (10.70): $P_e(t) = |\gamma_N|^2 \left| \int_0^t d\tau \exp[-i\bar{k}(t-\tau)] \phi(t-\tau) C_{ss}(\tau) \right|^2$; $C_{ss}(\tau)$ is the Fourier transform of $G_{ss}(E) = (E - E_s + (i/2)\Gamma_s)^{-1}$, where the total width of the $|s,\text{vac}\rangle$ state is the sum of the radiative and non-radiative widths $\gamma_s = \Gamma_s^r + \Gamma_s^{nr}$ and $\Gamma_s^{nr} = 2\pi |\langle s,\text{vac}|H_v|lc,\text{vac}\rangle|^2 \rho_c$ so that $C_{ss}(\tau) = \exp[-iE_s\tau - (\gamma_s/2)\tau]$. Thus we obtain

$$P_e(t) = |\gamma_N|^2 \frac{\exp(-\gamma_s t) + \exp(-\gamma_p t) - 2\exp[-(\gamma_s + \gamma_p)t/2] \cos(E_s - \bar{k})t}{(E_s - \bar{k})^2 + [(\gamma_p + \gamma_s)/2]^2} \tag{10.89}$$

From this result we conclude the following. (i) The only molecular information originating from the time evolution of this system is the resonance width Γ_s. Excitation characterised by different wave packet widths (i.e. different excitation times) would not result in a new information. (ii) The trigonometric factor $\cos(E_s - \bar{k})t$ in (10.89) represents a 'ringing effect' between the field and the molecular system. (iii) When $\gamma_p \gg \gamma_s$ we encounter the 'short excitation' condition (Section 10.9) whereupon $P_e(t) \propto \exp(-\gamma_s t)$. When both conditions (10.71) and (10.74) are obeyed the photon counting rate contains a single exponential decay $\dot{P}_\varphi(t) = \Gamma_s^r \exp(-\gamma_s t)$. Finally, the emission quantum yield is just the branching ratio between the radiative and the total widths $Y = \Gamma_s^r/\gamma_s = \Gamma_s^r/(\Gamma_s^r + \Gamma_s^c)$

10.11 CONSECUTIVE DECAY PROCESSES

Up to this point we have been concerned with simple coupling schemes where the intramolecular $\{|l\rangle\}$ manifold is not coupled to any additional decay channels. We have now to consider sequential decay processes where the doorway state (coupled to the radiative continuum) is also coupled to the (sparse or dense) $\{|l\rangle\}$ manifold which in turn is coupled to a final dissipative continuum. We consider first the physical situation where each of the intermediate $\{|l\rangle\}$ levels is coupled to a different final continuum, and thus exhibits non-interfering sequential decay (see Figure 10.6). Physical processes in this category are: (*a*) Sequential decay of the $\{|l\rangle\}$ quasi-continuum in an isolated statistical molecule owing to i.r. emission[30,78,123]. Thus each of the $|l,\text{vac}\rangle$ levels is coupled to a separate radiative continuum $|l',k_{l'}e\rangle$ where $|k_{l'}e\rangle$ corresponds to an i.r. photon. (*b*) Internal conversion in large molecules[55]. In the case of internal conversion from a highly excited singlet state the $\{|l,\text{vac}\rangle\}$ levels are electronically excited singlets, which are in turn radiatively coupled to highly excited (non totally symmetric) vibrational levels $|g\omega,k'e'\rangle$ of the ground electronic state. (*c*) Vibrational relaxation of the $\{|l\rangle\}$ manifold of a statistical molecule embedded in a medium[68]. In this case each $|l,\text{vac}\rangle$ level is separately coupled to a $|l'_{\{\omega_p\}},\text{vac}\rangle$ continuum containing a collection of medium phonon modes, characterised by the frequencies $\{\omega_p\}$. (*d*) Sequential electronic–vibrational relaxation of a small molecule[34]. As we have already pointed out, an isolated small molecule does not exhibit intramolecular electronic relaxation. However, when such a molecule is embedded in a dense medium, each individual level in the sparse manifold

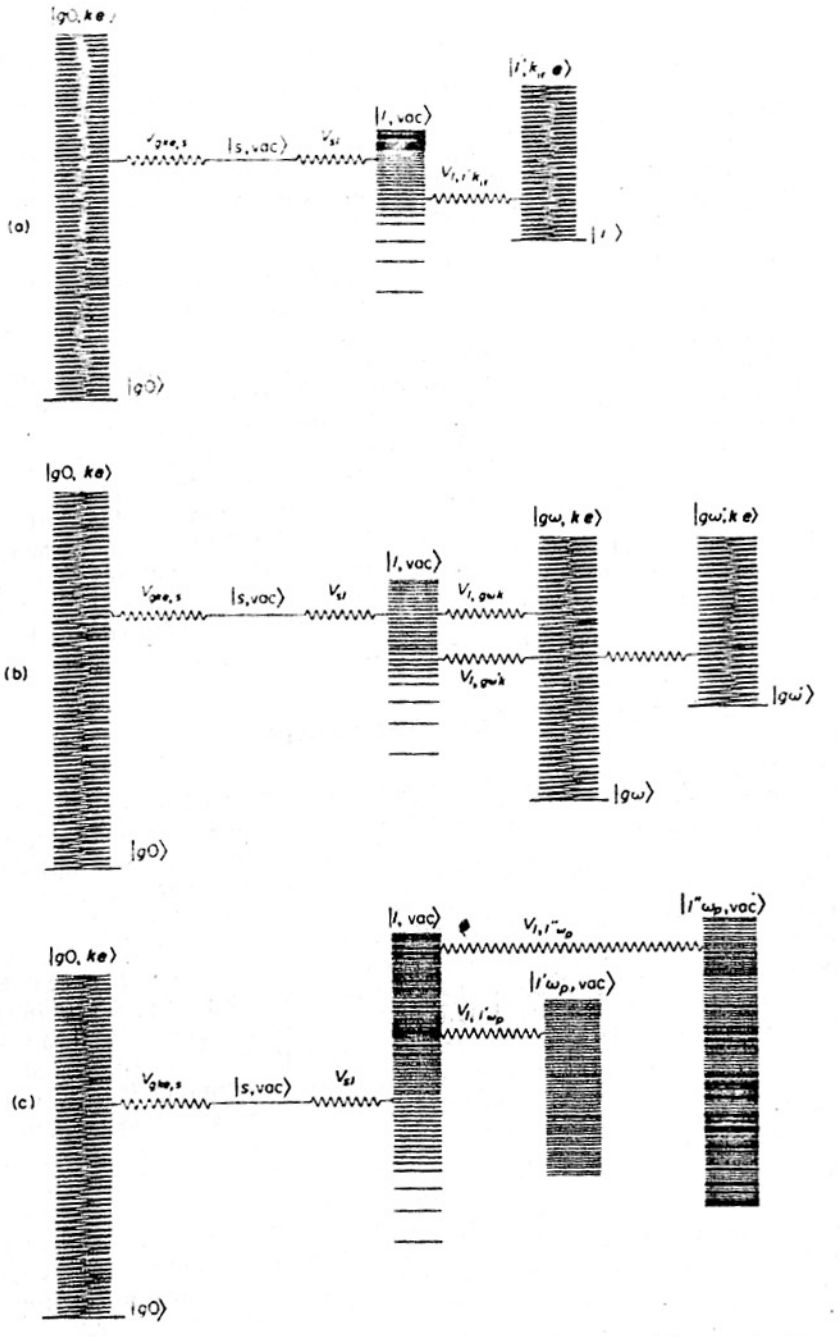

Figure 10.6 Sequential decay schemes. (a) Sequential decay of intramolecular continuum by i.r. emission. (b) Internal conversion. (c) Vibrational relaxation in the intramolecular manifold due to medium perturbation

$|l'$,vac$\rangle$ can subsequently decay via medium-induced vibrational relaxation to a lower level $|l_{\omega_{ll'}}$,vac$\rangle$, thus providing a pathway for the electronic-vibrational radiationless process. This process can be envisioned in terms of vibrational relaxation of the molecular eigenstates. (*e*) Sequential decay via a single level[54]. This is a model system where strong coupling is exhibited between the doorway state $|s$,vac$\rangle$ and one of the $|l$,vac$\rangle$ level. The special $|l\rangle$ level is subsequently coupled to an internal continuum. Such a physical situation is encountered for $S_1 \rightarrow T_1$ intersystem crossing with the participation of the T_2 levels[30].

We now proceed to outline the theory of non-interfering sequential decay. The energy levels of the system consist of a single resonance $|s$,vac$\rangle$ coupled in parallel to a radiative continuum $|g,\boldsymbol{ke}\rangle$ and to a quasi-continuum $\{|l$,vac$\rangle\}$. Each of the states in the $\{|l$,vac$\rangle\}$ manifold is in turn coupled to a separate continuum $\{|P_l\rangle\}$. Provided that the doorway state is 'initially excited' (see Section 10.9), the probability of finding the system in this state at time t is

$$P_s(t) = (4\pi)^{-2}\left|\int_{-\infty}^{\infty} \exp(-iEt)G_{ss}(E)\mathrm{d}E\right|^2 \tag{10.90}$$

while the probability the system be in any of the $\{|l$,vac$\rangle\}$ states is

$$P_l(t) = (4\pi)^{-2}\sum_l \left|\int_{-\infty}^{\infty} \exp(-iEt)G_{ls}(E)\mathrm{d}E\right|^2 \tag{10.91}$$

The diagonal matrix element of the Green function is

$$G_{ss}(E) = [E - E_s - \Delta_s^{nr} - \Delta_s + (i/2)\{\Gamma_s(E) + \Gamma_s^{nr}(E)\}]^{-1} \tag{10.92}$$

where Δ_s and Γ_s are the radiative level shift and width respectively, while the modified energy levels and the non-radiative contributions to the level shift operator are:

$$\tilde{E}_s = E_s + \Delta_s + \Delta_s^{nr}$$

$$\Delta_s^{nr} = \sum_l (E - \tilde{E}_l)|V_{sl}|^2/[(E - \tilde{E}_l^2) + (\Gamma_l/2)^2]$$

$$\Gamma_s^{nr}(E) = \sum_l \frac{\Gamma_l|\langle l,\mathrm{vac}|V|s,\mathrm{vac}\rangle|^2}{(E - \tilde{E}_l)^2 + (\Gamma_l/2)^2}$$

$$\tilde{E}_l = E_l + \mathrm{PP}\sum_{P_l} \frac{|\langle l,\mathrm{vac}|V|P_l\rangle|^2}{E - E_{P_l}}$$

$$\Gamma_l = 2\pi|\langle l,\mathrm{vac}|V|P_l\rangle|^2\rho_{P_l}(E_l) \tag{10.93}$$

Γ_l represents the width of each $\{|l$,vac$\rangle\}$ level owing to its coupling with the $\{|P_l\rangle\}$ continuum.

In general, the time evolution of the system may be very complex as the Green function (10.92) may be characterised by a large number of poles. However, under the extreme circumstances when the $\{|l\rangle\}$ manifold is sufficiently dense so that the widths Γ_l of these levels exceed their spacings,

$$\Gamma_l \gg |E_l - E_{l\pm1}| \approx \rho_l^{-1} \tag{10.94}$$

the function $\Gamma_s^{nr}(E)$ [equation (10.93)] is weakly varying with energy and may be considered to be constant around $E = E_c$. Under these circumstances G_{ss} has a single pole at $E = E_s - (i/2)(\Gamma_s^r + \Gamma_s^{nr})$. Thus the time evolution, equation (10.90), becomes

$$P_s(t) = \exp(-\gamma_s t) \tag{10.95}$$

being characterised by the total width

$$\gamma_s = \Gamma_s^r + \Gamma_s^{nr} \tag{10.96}$$

We can now inquire what is the probability for the population of the $\{|l,\text{vac}\rangle\}$ manifold. Utilising the Dyson equation, one obtains

$$G_{ls}(E) = \frac{\langle l,\text{vac}|V|s,\text{vac}\rangle}{E - \tilde{E}_l + (i/2)\Gamma_l} G_{ss}(E) \tag{10.97}$$

Now, provided the widths of the $|l\rangle$ states exceed their spacings according to (10.94), (10.97) together with (10.90) yield[75]

$$P_l(t) = \frac{\Gamma_s^{nr}}{\gamma_s - \Gamma_l}[\exp(-\Gamma_l t) - \exp(-\gamma_s t)] \tag{10.98}$$

This treatment results in the following conclusions:

(1) Equation (10.94) provides a necessary condition for treating an intra molecular quasi-continuum as a legitimate dissipative continuum.

(2) Equations (10.95) and (10.98) provide the time evolution for non-interfering sequential decay which involves an intermediate effective continuum $\{|l,\text{vac}\rangle\}$. The physical situation is adequately described by conventional kinetic expressions. This is the case for sequential decay of radioactive nuclei and of elementary particles[75].

(3) The decay of the doorway state is exponential and the decay rate (10.96) corresponds to parallel decay into a radiative and a non-radiative channel.

(4) The time evolution of the intermediate continuum represents a classical consecutive decay scheme, where the states in the $|l,\text{vac}\rangle$ manifold are populated by the decay of the doorway state and then exhibit subsequent decay.

These general results are of central importance for establishing the physical basis for the definition of the statistical limit (see Section 10.12). This formalism can be readily utilised for internal conversion[55], i.r. emission from large isolated molecules preceded by electronic relaxation[30,123] and medium-induced electronic–vibrational relaxation in a small molecule[68]. The physical situation is drastically different from the interesting case of sequential decay with interference, when all the states in the $\{|l\rangle\}$ manifold are coupled to a common continuum[70,124,125], when conventional kinetic schemes are no longer applicable. The latter case is applicable to Raman scattering from a dissociative molecular continuum[72] and to the interesting problems of photodissociation and predissociation of polyatomics[73]

10.12 THE STATISTICAL LIMIT

From the point of view of the working chemist, the formal theory of molecular relaxation phenomena is incomplete. To make the theoretical results

useful, real situations have to be treated. We now proceed to consider the details of the general theory of intramolecular electronic relaxation in large molecules and outline the analysis of some specific cases and examples.

10.12.1 Methodology

When the background density of vibronic levels in a large molecule is exceedingly high (see Figures 10.2 and 10.3 and Table 10.2) the intramolecular quasi-continuum does act as a practical decay channel. We have demonstrated that for a discrete spectrum $P_s(\infty) = 0$. Only when the system contains a real continuum is the emission quantum yield at the distant future lower than unity. These results do not contradict the idea of electronic relaxation (internal conversion or intersystem crossing) in an 'isolated' large molecule. The distinction between a 'real' (dissociative or ionisation) continuum and an intramolecular dense quasi-continuum is merely semantic, as one can always convert a 'real' continuum into a 'quasi-continuum' by imposing proper box normalisation boundary conditions which will not affect the experimental observables[41]. The concept of the statistical limit[30, 41] rests on two ideas. First, practical irreversibility of the intramolecular relaxation process on a timescale short relative to the (exceedingly long) Poincaré recurrence time for the system; and second, the occurrence of sequential decay processes in a dense intramolecular manifold. Bixon and Jortner[30] have introduced the notion of practical irreversibility in a simple model system where a single doorway state is coupled to an intramolecular quasi-continuum. As expected, the time evolution of the doorway state is given in terms of a Fourier sum which exhibits oscillatory behaviour. For the simple model system characterised by equal spacings, ρ_l^{-1}, between the states and by constant V_{sl} coupling terms, an exponential decay of the $|s\rangle$ state is exhibited, characterised by the decay rate $\Gamma_s^{nr} = 2\pi|V_{sl}|^2\rho_l$, on the timescale: $t \ll t_R = \hbar\rho_l$ [condition (a)]. This simple result establishes the timescale for the occurrence of effective relaxation into a quasi-continuum, introducing the notion of a Poincaré recurrence cycle for the decay process. For excited states of many large molecules, $\hbar\dot{\rho}_l$ is exceedingly long compared with all relevant decay times.

When the background level density is low, oscillatory decay resulting in quantum beats may be exhibited and no intramolecular relaxation due to this coupling occurs. A recent suggestion[126] concerning the possibility of observation of the first half-cycle of the Poincaré oscillation in the radiative decay of some excited molecular states corresponding to intermediate level structure (see Section 10.13.2) is fraught with conceptual difficulties, while tentative experimental observations may originate from time-resolved photon scattering by this complex multilevel molecular system which monitors the photon pulse shape, as is the case for the two-level system discussed in Section 10.6. Finally coherent (short time) excitation of a manifold corresponding to intermediate level structure may explain the experimental data.

In real life an 'isolated' molecule cannot wait long enough to pass a Poincaré cycle. Under any realistic experimental conditions the population of the $\{|l\rangle\}$ manifold is relaxed owing to 'trivial' quenching processes such as wall collisions or gas kinetic collisions. Finally, it is important to realise that

even an isolated large molecule under 'astrophysical' conditions in the absence of 'trivial' quenching mechanisms would not exhibit a Poincaré cycle. In a real molecule the $\{|l\rangle\}$ manifold exhibits subsequent decay mechanisms, such as i.r. emission to lower vibrational levels[30,78], or radiative decay to the highly vibrationally-excited ground state levels in the case of internal conversion[33,78,55] between highly excited states. Thus, strictly speaking, all electronic relaxation processes in a large molecule involve non-interfering sequential decay. Following the treatment of Section 10.11 it is immediately apparent that provided the widths Γ_l exceed their spacings, i.e. $\Gamma_l \gg \rho_l^{-1}$ [condition (b)], the intramolecular quasi-continuum acts as a dissipation channel. The decay rate of the doorway state $\gamma_s = \Gamma_s^r + \Gamma_s^{nr}$ consists of a sum of radiative and non-radiative contributions.

Conditions (a) and (b) provide the physical basis for the definition of the statistical limit in a large molecule. Each of these relations yields an independent necessary and sufficient condition for treating the intramolecular quasi-continuum as a legitimate dissipative continuum. When condition (a) is satisfied and the widths Γ_l are very small (originating from i.r. decay, as will be the case for intersystem crossing) we can set $\Gamma_l \to 0$ in (10.93) whereupon

$$\Gamma_s^{nr} = 2\pi \sum_l |V_{sl}|^2 \, \delta(E - \tilde{E}_l) \tag{10.99}$$

which is the conventional expression for the non-radiative decay probability into a continuum[22,47,48], the delta function entering as a book-keeping device. When only condition (b) is satisfied, as may be the case for internal conversion, or for electronic–vibrational relaxation, (10.93) has to be used.

The physical situation in the statistical limit is that of a parallel decay of a single discrete level into two non-interacting channels. The photon counting rate is $I(t) = \Gamma_s^r \exp(-\gamma_s t)$ while the quantum yield is $Y = \Gamma_s^r/(\Gamma_s^r + \Gamma_s^{nr})$. These results constitute conventional kinetic rate expressions. The decay rate γ_s exceeds the radiative width Γ_s^r, which can be evaluated from the integrated oscillator strength, the decay mode resulting from short-time excitation consists of a single exponential, and the emission quantum yield is lower than unity. These features of the radiative decay of many excited states of large molecules in solution are well documented[8-15]. More interesting is the theoretical argument for the occurrence of electronic relaxation in an isolated large molecule[127,132]. An inert medium (see Section 10.12.3) does not modify the decay rate γ_s in a statistical molecule. Medium-induced vibrational relaxation just introduces an additional contribution to the width Γ_l, equation (10.93). When $\Gamma_s^{nr}(E)$ is already a slowly varying function of the energy in the isolated molecule, this additional sequential decay process is of minor importance. Experimental evidence regarding this cardinal point is rather sparse and we have summarised in Table 10.4 the available information regarding the decay characteristics of the first excited singlet states of anthracene and of azulene which are practically invariant to inert solvent perturbations, in accord with the theoretical predictions. In view of medium-induced vibrational relaxation in the singlet manifold, such comparison between the 'isolated' and the medium-perturbed molecule should in fact be performed for the zeroth vibronic level. Finally, we would like to point out that the only

Table 10.4 Non-radiative decay times of some statistical molecules in the gas phase and in solution

Molecule	*Decaying state* *	τ_{nr}/sec †		Y	
		Solution	*Gas phase*	*Solution*	*Gas phase*
Anthracene	$^1B_{2u}(S_1)$	7.5×10^{-9} ‡§	7.5×10^{-9} §	0.36 ‡	0.4 §
Azulene	$^1B_1(S_1)$	7.5×10^{-12} ‖	2.5×10^{-12} ••	$\sim 10^{-6}$ ‖	10^{-6} ¶
		3×10^{-12} ¶	3×10^{-12} ••		

* Data both for solution and gas phase refer to low vibronic component of the given electronic state
† $\Gamma_{nr} = \tau_{nr}^{-1}$
‡ Berlman, I. (1965). *Handbook of Fluorescence Spectra* (New York: Academic Press)
§ Tsernichovsky, N. and Jortner, J. Unpublished data
‖ Rentzepis[166]
¶ τ_{nr} from Y data of Ref. 132
•• Direct relaxation measurements of Huppert, D. (1974). *Ph.D. Thesis.*, Tel-Aviv University

pertinent molecular information originating from the study of the decay of a statistical molecule is the resonance width γ, and one cannot obtain any new information regarding the decay characteristics of the system by changing the parameters of the exciting photon wave packet.

10.12.2 Energy dependence of non-radiative decay

The general approach to the statistical limit outlined above provides only qualitative, general information, which may be viewed with some suspicion by the experimentalist. Only a limited number of genuine theoretical calculations have been performed up to date[68,104,133,138]. We discuss first the analysis of the non-radiative decay of individual vibronic levels of a large molecule as a function of excess vibrational energy[49,53,58,59,134-147], comparing these results with some experimental data on optical selection studies. We focus attention on electronic relaxation in a two-electronic-level system, $|s\rangle$ and $|l\rangle$, bearing in mind that the optically accessible zero order states do not involve just a single doorway state but rather a manifold $|sI\rangle$ of vibronic levels corresponding to the $|s\rangle$ type excited electronic configuration, each of which may be considered to decay independently. Here $|I\rangle$ refers to the collective vibrational state. The non-radiative decay rate $|sI\rangle \rightarrow \{|l\rangle\}$ of a single vibronic level may be expressed[58,59] in terms of the Franck–Condon vibrational overlap integrals, or alternatively, by utilising the Feynman operator techniques. Adopting the latter elegant approach, (10.99) can be recast in terms of the Fourier integral of a generating function,

$$\Gamma_{sI}^{nr} = (2\pi)^{-1}\int_{-\infty}^{\infty} d\tau \exp(-i\Delta E\tau)L(\tau)$$

$$L(\tau) = \langle I|V_{sl}\exp(ih_l\tau)V_{sl}^{\dagger}\exp(-ih_s\tau|)I\rangle \qquad (10.100)$$

where $\Delta E = E_{s0} - E_{l0}$ is the electronic energy gap and h_l and h_s correspond to the adiabatic Hamiltonians for the nuclear motion in the two electronic states. For a harmonic molecule, $|I\rangle = \prod_{\mu}|\mu_{\cdot}\rangle$. Consider two potential surfaces, Figure 10.7, of such a harmonic molecule, characterised by the normal coordinates $\{Q_{\mu}^{(\alpha)}\}$, equilibrium configuration $\{Q_{\mu 0}^{(\alpha)}\}$, reduced masses $\{M_{\mu}^{(\alpha)}\}$ and frequencies $\{\omega_{\mu}^{(\alpha)}\}$, where the subscript $(\alpha) \equiv s,l$ labels the electronic states. The configurational changes are due to the different equilibrium configurations in the two states, i.e. $Q_{\mu 0}^{(s)} \neq Q_{\mu 0}^{(l)}$ for some μ. The (dimensionless) configurational distortion parameters which specify the relative displacements of origins are $\Delta\mu = (M_{\mu}\omega_{\mu}/\hbar)^{\frac{1}{2}}(Q_{\mu 0}^{(s)} - Q_{\mu 0}^{(l)})$. The excess vibrational energy in this model is $E_v = \sum_{\mu}(v_{\mu} + \frac{1}{2})\hbar\omega_{\mu}$, v_{μ} being the vibrational quantum number in the μth mode. Now, in the weak-coupling situation the generating function, equation (10.100) can be separated into a sum of contributions from different promoting modes. We believe that this physical situation applies for most electronic relaxation processes.

Numerical calculations based on the harmonic models for a large molecule lead to several general trends[59]. First, for a large electronic energy gap,

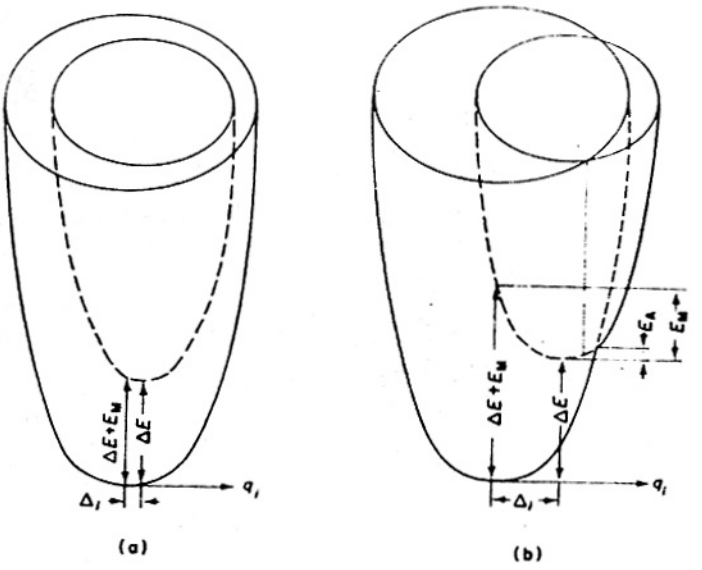

Figure 10.7 Schematic representation of the two adiabatic potential surfaces in two-dimensional vibrational space. (a) The weak coupling limit. (b) The strong electron–phonon coupling case

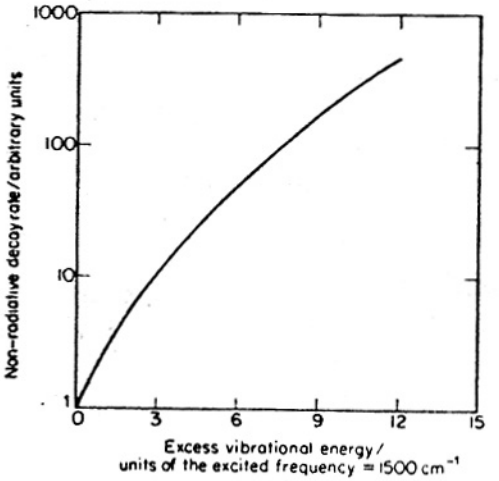

Figure 10.8 Non-radiative decay rate as a function of the excess vibrational energy for a large electronic energy gap. The model molecule is characterised by the accepting modes: $\omega_1 = 3000\ cm^{-1}$, $\omega_2 = 1500\ cm^{-1}$, $\Delta_1 = 0.8$, $\Delta_2 = 1.0$; $\Delta E_{eg} = 30\,000\ cm^{-1}$. ω_2 is taken to be the optically excited frequency

$\Gamma^{nr}_{vj}(E_v)$ exhibits a fast, close to exponential, increase with E_v (see Figure 10.8). Such a situation was observed for 'optical selection' studies in β-naphthylamine[143]. Second, for moderate $\Delta E \sim 6000$–$7000\ cm^{-1}$ energy gaps, $\Gamma^{nr}_{vj}(E_v)$ exhibits a slow (close to linear) increase with E_v (see Figure 10.9). The most extensively studied case involves the $^1B_{2u} \rightarrow {}^3B_{1u}$ intersystem crossing in benzene[140-142, 144] (see Table 10.5). Adopting a brute-force method of calculating Franck–Condon factors, Heller *et al.*[138] obtained qualitative agreement between experiment and theory, accounting not only for the general trend but also for the more detailed effects regarding the nature of the particular vibronic levels. Third, for small electronic energy gaps $\Delta E < 5000\ cm^{-1}$, a new effect is expected and $\Gamma^{nr}_{vj}(E_v)$ should decrease with increasing E_v. This reversal effect exhibited in Figure 10.9 originates from the contribution of Franck–Condon overlaps at low ΔE. It should be

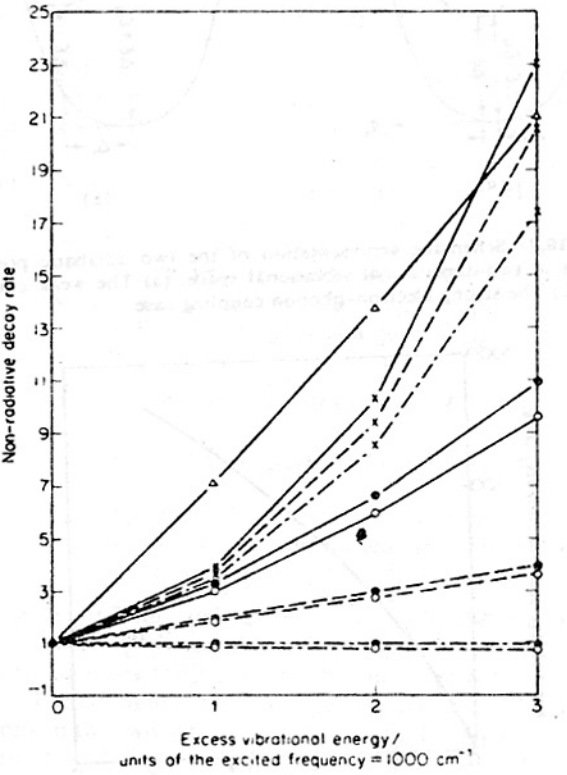

Figure 10.9 Non-radiative decay rate as a function of the excess vibrational energy for moderate electronic energy gaps. The model molecule is characterised by the accepting modes: $\omega_1 = 1000\ cm^{-1}$, $\omega_2 = 3000\ cm^{-1}$. ω_1 is taken to be the optically excited frequency. — · — · —, $\Delta E = 6000\ cm^{-1}$; — — —, $\Delta E = 7000\ cm^{-1}$; ——, $\Delta E = 7000\ cm^{-1}$; ○, $\Delta_1 = 0.24$, $\Delta_2 = 0.071$; △, $\Delta_1 = 0.24$, $\Delta_2 = 0.6$; ●, $\Delta_1 = 0.1$, $\Delta_2 = 0.071$; ×, $\Delta_1 = 0.9$, $\Delta_2 = 0.071$

Table 10.5 Optical selection studies in benzene. Data correspond to the relative non-radiative rates for the $6^{-1}1^{x}$ progression in the $^1B_{2u}$ state

	C_6H_6			C_6D_6		
Optically selected state	E_v/ cm^{-1} *	*Experiment* †	*Calculated*	E_v/ cm^{-1} *	*Experiment* ‡	*Calculated*
6^01^0	0	1.00 §	1.00	0	1.00 §	1.00
6^11^0	521	1.19	1.14	498	1.24	1.22
6^01^1	923	1.22	1.27	879	1.55	1.59
6^21^0	1040	1.27	1.32	996	1.36	1.52
6^11^1	1444	1.42	1.45	1377	1.92	1.93
6^01^2	1846	1.73	1.62	1758	2.69	2.49
6^21^1	1965	1.64	1.67	1875	2.89	2.39
6^11^2	2367	1.94	1.84	2256	3.64	3.00
6^01^3	2769	2.42	2.05	2637	3.64	3.82
6^21^2	2882	2.67	2.12	2754	5.15	3.71

* Excess vibrational energy above $^1B_{2u}$ ($v = 0$) state.

† Spears and Rice[144a]

‡ Abramson, Spears and Rice[144b]

§ $\tau_{nr}(v = 0) = 128$ ns for C_6H_6[144a] and $\tau_{nr}(v = 0) = 309$ ns for C_6D_6[144a]

‖ Calculated by Heller, Freed and Gelbart[138] from the harmonic model with the following input data: C_6H_6: $\Delta E = 8200$, $\omega_x = 1500$, $\omega_1 = 923$, $\omega_6 = 521$, $\omega_M = 3130$; $\mathcal{A}^2_1/2 = 0.025$, $\mathcal{A}_6 = 0$; $\mathcal{A}_M^2/2 = 0.0020$; $\Delta\omega_1 = 25$; $\Delta\omega_6 = 50$. C_6D_6: $\Delta E = 8200$, $\omega_x = 1440$, $\omega_1 = 879$, $\omega_6 = 499$; $\omega_M = 2340$, $\mathcal{A}_M^2/2 = 0.0028$. All other data same as those for C_6H_6. Frequencies ω_i and frequency changes given in cm^{-1}.

stressed, however, that this reversal effect is difficult to observe experimentally, as for small ΔE values the excited state does not correspond any more to the statistical limit. When a large molecule with an excited state which corresponds to such an intermediate situation (see Section 10.13.2) is embedded in a dense medium it exhibits electronic relaxation due to consecutive interstate coupling, followed by medium-induced vibrational relaxation. We have to find a rather extreme case where the medium-enhanced electronic relaxation is faster than the vibrational relaxation rate. Such a case is provided by the $S_1 \rightarrow T_1$ intersystem crossing of benzophenone ($\Delta E \approx 3000\ \text{cm}^{-1}$) in solution where (see Figure 10.10) Rentzepis[53,148] has observed $\omega_{s4}/\omega_{s0} = 0.4$, in accord with theoretical predictions.

In the foregoing discussion we have endorsed the point of view that anharmonic intrastate vibrational-energy relaxation in an isolated large molecule is of minor importance. Fischer's claim[135,149,150] that an isolated large molecule can act as its own heat bath is not supported by experimental or theoretical evidence for optical selection studies in the S_1 state of benzene[140-142,144] and naphthalene[146] at moderate $E_v \approx (3\text{–}5) \times 10^3\ \text{cm}^{-1}$ excess vibrational energies. It is important to notice that the erosion of the structure in the Γ_{s1} *versus* E_v curve for different molecules larger than naphthalene does not necessarily imply intrastate vibrational energy redistribution, as sequence congestion effects[68] may contribute to this phenomenon.

The optical selection studies discussed above involve electronic relaxation between excited states. Electronic relaxation to the ground state may be of considerable importance in photochemical processes. In this case a highly vibrationally excited ground state is produced which may undergo (i)

isomerisation to a vibrationally hot ground state, as in some trienes[151], or (ii) may exhibit vibrational predissociation as in the case of formaldehyde[152]. The preparation of the reactive state is drastically different in thermal reactions. The case of the benzene molecule[144] is of great interest, as it exhibits a sharp drop in the Y and in $\Gamma_{vl}(E_v)$ for $E_v > 3000\,\text{cm}^{-1}$ above the $^1B_{2u}$ state, which was attributed to case (ii), but a careful negative search for photofragments[153] indicates that case (i) applies here. Internal conversion to the ground state should be a sharply increasing exponential function of E_v.

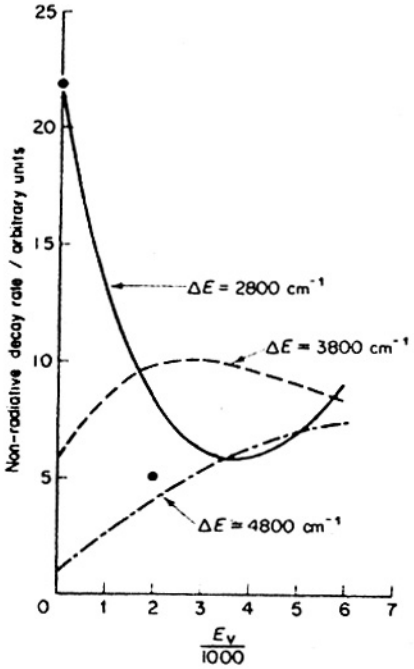

Figure 10.10 Reversal effect of the non-radiative decay rate as a function of excess vibrational energy. Model calculations performed for a model molecule with $\Delta_1 = \Delta_2 = 0.7$, $\omega_1 = 1000\,\text{cm}^{-1}$, $\omega_2 = 3000\,\text{cm}^{-1}$. ——, $\Delta E = 2800\,\text{cm}^{-1}$, — — —, $\Delta E = 3800\,\text{cm}^{-1}$ and —.—, $\Delta E = 4800\,\text{cm}^{-1}$. The two dots represent the experimental data of Rentzepis[148] for $S_1 \rightarrow T_1$ non-radiative decay of benzophenone in solution

The role of electronic relaxations as precursor processes for photochemical reactions is crucial and not yet well understood. Vibronic photochemistry from optically selected levels in the gas phase should provide basic information on primary photochemical paths. In the study of the photochemistry of the $^1A_2$ (Π) state of cyclobutanone[154] as a function of E_v at moderately low pressures, it was found that the fluorescence lifetimes decrease exponentially together with Y for up to $E_v = 1900\,\text{cm}^{-1}$. This is interpreted as process (ii) although the benzene situation calls for some caution. The photochemistry in this energy range exhibits two channels:

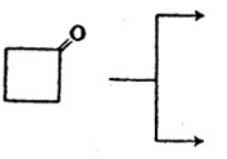

$$\rightarrow CH_2{=}CH_2 + CH_2{=}C{=}O \qquad [C_2]$$

$$\rightarrow \triangle + CO \qquad [C_3]$$

The $[C_3]/[C_2]$ ratio decreases with increasing E_e. We conjecture that the increase in ω_{sI} and the increase in the $[C_2]$ product with increasing E_e originates from the dramatic enhancement of intersystem crossing to the (vibrationally hot) ground state, which subsequently predissociates by vibration. This is consistent with our model calculations[53] for optical selection for large ΔE ($\sim 30\,000\ \mathrm{cm}^{-1}$) values. On the other hand, the $[C_3]$ product may originate via intersystem crossing to the triplet state. In view of the lower ΔE value the rate for this process should increase relatively slowly with increasing E_e.

10.12.3 The energy gap law and related phenomena

To make the theory of electronic relaxation in the statistical limit really useful, algorithms have to be devised to specify general characteristics of the decay problem. Several authors[47, 48, 99, 150, 155] have developed the formalism of multiphonon molecular processes for the study of non-radiative widths, thus expressing the decay probability in terms of a generalised lineshape function[22] in the limit of zero frequency. The molecule is embedded in an inert medium[34, 48] which does not modify the molecular energy levels, does not enhance the intramolecular coupling (by affecting spin–orbit coupling) and does not contribute new states, such as charge transfer states. This inert medium just provides a heat bath for (fast) vibrational excitation and relaxation within the $|sI\rangle$ states. The thermally-averaged non-radiative decay rate is

$$\langle \Gamma \rangle_T = \frac{\sum_I \exp(-E_{sI}/kT)\Gamma_{sI}^{\mathrm{nr}}}{\sum_I \exp(-E_{sI}/kT)} \qquad (10.101)$$

where $\Gamma_{sI}^{\mathrm{nr}}$ is given by (10.99). General methods for handling weighted densities of states of this form have been provided in solid state physics[22]. These techniques are limited for the case of a harmonic molecule, or for the case when only a single mode is strongly anharmonic (i.e. *cis–trans* isomerisation[20] or thermally induced photodissociation[17]), where all the other modes are taken to be harmonic. In the former case one can utilise (10.100) together with (10.101) to express $\langle \Gamma \rangle_T$; the same result is obtained using the density matrix for the harmonic oscillator. The electron–phonon coupling is specified in terms of the coupling strength $g = \frac{1}{2}\sum_\mu \Delta_\mu^2 (2\langle n_\mu \rangle + 1)$, $\langle n_\mu \rangle$ being the thermal phonon occupation number. Two limiting situations[47, 48] can be considered which are portrayed in Figure 10.6. The strong-coupling situation is characterised by large relative displacements of the potential surfaces, i.e. $g \gg 1$, and the weak coupling limit specified by small relative displacements, whereupon $g \ll 1$.

The strong-coupling situation involves non-adiabatic curve-crossing not far from the minimum of the potential curve $U_s(Q_j)$ of this state. At high temperatures ($kT \gg \hbar\omega_\mu$) the quantum mechanical treatment results in an activated rate expression $\langle \Gamma \rangle_T \propto \exp(-E_A/kT)$ where the activation energy,

E_A, corresponds to the minimum on the hypersurface of intersection of $U_3(Q^{(1)})$ and $U_2(Q^{(1)})$ relative to the energy $U_1(Q_{,0}^{(1)})$. Furthermore, a weak deuterium isotope effect on Γ_T is expected. This state of affairs is highly relevant for photochemical rearrangement reactions and also for some solid-state problems, such as thermal ionisation of impurity centres in semiconductors[22], or for chemical electron transfer reactions in ionic solutions[27]. The harmonic model should be drastically modified to study photochemical rearrangements involving large configurational changes[20,21] in excited electronic states of large molecules which usually occur along a single coordinate, which cannot be taken to be harmonic.

In the weak-coupling situation, (10.101) for a harmonic molecule can be approximated using the saddle point method, resulting in the form[47]

$$\langle \Gamma \rangle_T \propto \exp(-\gamma \Delta E/\hbar\omega_M) \tag{10.102}$$

for large values of ΔE, the electronic energy gap. Here $\hbar\omega_M$ is the maximum molecular frequency (i.e. $\hbar\omega_M \approx 3000\ \mathrm{cm}^{-1}$ for C_nH_n and $\hbar\omega_M \approx 2200\ \mathrm{cm}^{-1}$ for C_nD_m aromatic hydrocarbons). γ is a weakly varying function of Δ_μ, ω_M and ΔE, being ~ 1–2. More detailed calculations[48] demonstrate that ΔE in (10.102) has to be modified in two ways. First, ΔE has to be replaced by $(\Delta E - \hbar\omega_z) = \Delta E_z$, accounting for the excitation of a promoting mode. Second, the energy gap has to incorporate the differences between the zero-point energies in the two electronic states. These modifications do not affect general relations and correlations within a class of similar systems. Equation (10.102) exhibits two important characteristics; first, the energy-gap law for electronic relaxation, and second, the deuterium isotope effect[156] on $\langle \Gamma \rangle_T$, both of which concur with the gross features of experimental observations. The energy-gap law, originally invoked by Robinson and Frosch[5], is well documented for the internal conversion from the first triplet state of aromatic hydrocarbons[158]. A recent demonstration for the $S_2 \rightarrow S_1$ internal conversion in a series of azulene derivatives[159] where $\gamma \approx 3$ is portrayed in Figure 10.11. Figure 10.12 exhibits a more interesting case, the energy-gap law for electronic relaxation between electronic states of rare-earth ions in ionic crystals[160-163] where the impurity ion together with the crystal phonon field constitutes a 'statistical' supermolecule.

The temperature dependence of electronic relaxation in aromatic hydrocarbons in an inert medium about and below room temperature originates[48,99,138] from the thermal population of the promoting modes. High-frequency accepting modes are not thermally excited. For the case of transition metal ions, thermal effects are much more pronounced in view of the low value of the phonon frequencies and can be recast in the form[160-163],

$$\langle \Gamma \rangle_T = \Gamma_{T=0}(1 + \langle n_m \rangle_T)^{\Delta E/\hbar\omega_M} \times \exp\left(-\sum_m L_m \langle n_m \rangle_T \Delta_m^2/2\right) \tag{10.103}$$

where the index m specifies an effective mode of frequency ω_m and degeneracy L_m, which lies close to the maximum phonon ($\omega_m \sim 150\ \mathrm{cm}^{-1}$), $\langle n_m \rangle_T$ is the thermally averaged occupation number of this mode. The temperature effect in (10.103) originates from two contributions, a spontaneous and stimulated process involving the emission of p phonons resulting in the $(1 + \langle n_m \rangle_T)^p$

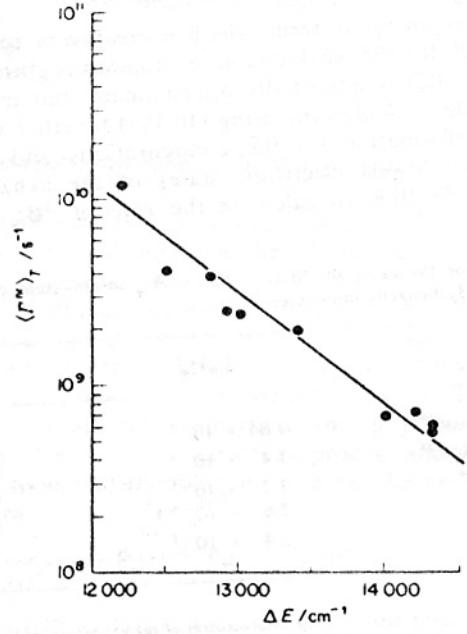

Figure 10.11 The energy gap law for $S_2 \rightarrow S_1$ relaxation of azulene derivatives. (Data from Ref. 159, by courtesy of Verlag Chemie.)

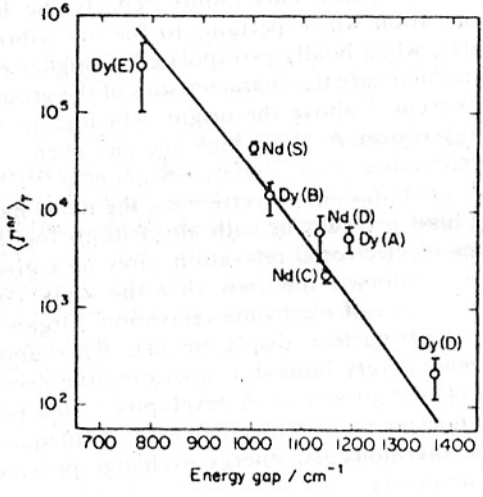

Figure 10.12 The energy-gap law for electronic relaxation of excited rare earth ions in $LaCl_3$. (Adopted from Fong, Naberhuis and Miller[162], by courtesy of the American Institute of Physics.)

term and the exponential term which corresponds to the Debye Waller factor and which for the weak-coupling situation is close to unity.

Equation (10.102) is admittedly approximate, but useful for qualitative purposes. Detailed calculations using (10.101) together with all the detailed spectroscopic information on the configurations and frequency changes between the two lowest electronic states of the benzene molecule were utilised, see Table 10.6, to calculate the rate of $^3B_{1u} \rightarrow {}^1A_{1g}$ intersystem

Table 10.6 Data for the rates of $^3B_1(v = 0) \rightarrow {}^1A_{1g}$ intersystem crossing in the benzene and [$^2H_6$]benzene molecules*

	C_6H_6	C_6D_6
Burland and Robinson[104]	9.04×10^{-5}	1.18×10^{-10}
Fischer and Schneider[133]	7.4×10^{-4}	3.1×10^{-5}
Nitzan and Jortner[68]	7.2×10^{-7}	6.6×10^{-11}
	2.6×10^{-5} †	1.2×10^{-10} †
Experiment[104]	2.4×10^{-2}	—

* Rates in s^{-1}

† Using Fischer and Schneider's data[133] for the displacement of the e_{2g} deformation mode

crossing in benzene. These detailed results confirm the energy-gap law $\ln \omega \propto (\Delta E/3000\ \mathrm{cm}^{-1})$ and the deuterium isotope effect; however, the absolute value of $\omega(C_6H_6)$ is lower by about 2–3 orders of magnitude from the experimental result. This failure reflects the limitations of the spectroscopic information which pertains to the low vibronic levels of the two electronic states, when boldly extrapolated to higher energies. We have to know in this particular case the characteristics of the ground-state potential surface about 30 000 cm^{-1} above the origin, which cannot be extrapolated from the low-energy region. At these high energies even first (or low) order anharmonicity corrections as attempted by Fischer *et al.*[133,164] are inapplicable and a new approach is required. Nevertheless, the naive harmonic model in the weak-coupling limit provides us with alogarithms for the description of the general features of electronic relaxation rates in a given class of large molecules. We have endorsed the view that the weak coupling situation is adequate for most cases of electronic relaxation. Organic photochemical processes involve large nuclear displacements, whereupon spectroscopic information is in general very limited in providing the necessary input data for the elucidation of such processes. A development of a proper description of large amplitude nuclear motion together with an adequate description of intramolecular and intermolecular energy exchange provides the next outstanding goals of the theory.

We have focused attention on the case of thermally averaged decay which in the low-temperature limit (when $kT \ll \hbar\omega_\mu$ for all μ) reduces to Γ_{s0}^{nr}. When a molecule is externally perturbed, coupling between electronic and vibrational relaxation[65] should be considered. Such processes are of central importance for the understanding of some experimental results of picosecond

spectroscopy in solution[148] and also for collision-induced vibrational relaxation[165] in the gas phase.

10.12.4 Internal conversion in the statistical limit

In the case of internal conversion[55] between highly excited singlet states $|s,\text{vac}\rangle$ in a statistical molecule, the $\{|l,\text{vac}\rangle\}$ quasi-continuum states correspond to electronically excited levels of the same spin multiplicity as the doorway state. The $\{|l,\text{vac}\rangle\}$ states carry oscillator strength to highly vibrationally excited $|glw,ke\rangle$ levels of the ground state (see Figure 10.5). In view of symmetry restrictions on the vibrational part of $|l,\text{vac}\rangle$, which have to contain a promoting mode, each of the final $|glw\rangle$ levels has to be characterised by the same vibrational symmetry as the $\{|l\rangle\}$ excited states. This physical situation involves a sequential decay process and was discussed in Section 10.11. The total photon counting rate can be expressed as a sum of two contributions

$$\dot{P}_g(t) = \dot{P}_s(t) + \dot{P}_l(t) = \Gamma_s^r|C_s^r(t)|^2 + \sum_l \Gamma_l^r|C_l(t)|^2 \qquad (10.104)$$

where Γ_s^r and Γ_l^r correspond to the radiative width of the zero order $|s,\text{vac}\rangle$ and $|l,\text{vac}\rangle$ states, respectively. The first term in (10.104) corresponds to the $|s,\text{vac}\rangle \rightarrow |g0,ke\rangle$ emission (the s region) while the second term represents the ($|l,\text{vac}\rangle \rightarrow |glw,ke\rangle$) radiative decay (the l region). In the statistical limit we can safely assume that the s and l regions are well separated in energy. The decay rates are $\dot{P}_s(t) = \Gamma_s^r \exp(-\gamma_s t)$ in the s region, where γ_s is given by (10.96), and

$$\dot{P}_l(t) = \frac{\Gamma_l^r \Gamma_s^{nr}}{\gamma_s - \Gamma_l^r}\left\{\exp(-\Gamma_l^r t) - \exp(-\gamma_s t)\right\}$$

in the l region. These are conventional kinetic results for sequential decay. The radiative decay in the s region is exponential, exhibiting the lifetime $(\Gamma_s^r + \Gamma_s^{nr})^{-1}$ and the quantum yield $Y_s = \Gamma_s^r/(\Gamma_s^r + \Gamma_s^{nr})$, as in the conventional case of the statistical limit. The radiative decay in the l region originates from the $|l\rangle \rightarrow |glw,ke\rangle$ transition from highly excited vibrational states. The decay pattern exhibits a short-time built up component $\dot{P}_l(t \rightarrow 0) \approx \Gamma_l^r \Gamma_s^{nr} t$ and a long-time decay behaviour $\dot{P}_l(t) \rightarrow \exp(-\Gamma_l^r t)$. The total quantum yield in the l region is $Y_l = \Gamma_s^{nr}/\gamma_s$. We note that the experimental decay modes in the two regions are appreciably different, consisting of a high-energy short lifetime range and a low-energy long lifetime region. Finally, we emphasise that in this physically realistic example for the statistical limit no interference effects in the radiative decay will be exhibited.

10.13 INTERSTATE COUPLING IN POLYATOMIC MOLECULES

It is of crucial importance to distinguish between the effect of interstate coupling which occurs, in principle, in all polyatomic molecules irrespective

of the density of background states, and the phenomenon of intramolecular relaxation, which is exhibited only in the statistical limit. In this section some of the implications of interstate scrambling are discussed.

10.13.1 The small molecule case

In the small molecule limit[32, 33, 113] the interstate coupling matrix elements V_{sl} between the Born–Oppenheimer states are large while the density of states in the background manifold is low (see Table 10.2). As the $|l\rangle$ levels are coarsely spaced relative to their radiative widths, the sparse $\{|l\rangle\}$ manifold cannot act as a dissipative channel in the isolated molecule and we have to consider the problem of the radiative decay for a set of discrete, coupled levels, i.e. $|s,\text{vac}\rangle$ and $|l,\text{vac}\rangle$. Now, the level distribution of the molecular eigenstates is sufficiently sparse so that in the absence of accidental degeneracies we expect the off-diagonal matrix elements of the radiative decay matrix to be negligible, compared with the level spacings, i.e. $\Gamma_{nn'} \ll |E_n - E_{n'}|$. Thus, H_{eff} in the ME, $|n,\text{vac}\rangle$, representation is diagonal. Under these circumstances the molecular eigenstates are expected to provide a good description of the independently decaying levels $|j,\text{vac}\rangle$. The corresponding complex energies are $(H_{\text{eff}})_{nn'} = (E_n - i\Gamma_n/2)\delta_{nn'}$, where the radiative widths of the molecular eigenstates are just

$$\Gamma_n^r = \Gamma_s^r |\langle s,\text{vac}|n,\text{vac}\rangle|^2 \tag{10.105}$$

and Γ_s^r is the radiative width of the 'doorway state'. In view of the diagonal sum rule, $\Gamma_s^r = \sum_n \Gamma_n^r$, thus $\Gamma_n \ll \Gamma_s$ for all n. The factors $|\langle s,\text{vac}|n,\text{vac}\rangle|^{-2}$ are of the order of the number of effectively coupled levels in the $\{|l\rangle\}$ manifold. These considerations provide a coherent explanation for the anomalously long radiative decay times compared with what is expected on the basis of the integrated oscillator strength of small molecules[113] (see Table 10.7). The occurrence of interstate coupling in small molecules results from the distribution of the absorption intensity of the doorway state and the dilution of its decay time among the molecular eigenstates, each of which is active in absorption and in emission. We also note that in this case of a discrete

Table 10.7 Long radiative lifetimes of small molecules

Molecule	*Transition*	τ(exp)/s	τ(integrated *f*)/sec
NO_2	$^1B_2$–$^1A_1$ 4300 Å	44×10^{-6}	0.3×10^{-6}
SO_2	$^1B_1$–$^1A_1$ 3000 Å	42×10^{-6}	0.2×10^{-6}
CS_2	$^1\Sigma$–$^1\Sigma$ $^1\Pi$–$^1\Pi$ 3200 Å	15×10^{-6}	3×10^{-6}

* Experimental results for τ(exp) from Douglas[113]

spectrum we expect that $\Gamma \gg \Gamma^{166}$. The photon counting rate under excitation conditions corresponding to a Lorentzian pulse with $\gamma_p \gg \gamma_n$ for all n is

$$I(t) \propto \sum_n \frac{\Gamma_n^r}{(\bar{k} - E_n)^2 + (\gamma_p/2)^2} \exp(-\Gamma_n^r t) \tag{10.106}$$

whereupon the decay mode is in general a superposition of exponentials. The constant coefficients in (10.106) just express the absorption strength of the wave packet by the individual molecular eigenstates.

The isolated small-molecule case corresponds essentially to excitation and decay from the molecular eigenstates and it is meaningless to consider non-radiative relaxation from $|s\rangle$ to $|l\rangle$ in the isolated small molecule. Only when such a small molecule is embedded in a medium, sequential electronic medium-induced vibrational relaxation may result in non-radiative relaxation of the doorway state[34]. Adopting the theory of sequential decay, the (initial) non-radiative decay rate of a doorway state of a small molecule in an inert medium is[34]

$$\omega_{sl} = \sum_j \frac{|\langle si|H_v|lj\rangle|^2 \Gamma_{lj}}{(E_{sl} - E_{lj})^2 + (\Gamma_{lj}/2)^2} \tag{10.107}$$

where Γ_{lj} is the width of the $|lj\rangle$ background state owing to vibrational relaxation. It is amusing to notice that in the case of degeneracy (where the present theory has to be extended), $\omega_{sl} \approx |\langle si|H_v|lj\rangle|^2/\langle\Gamma_l\rangle$, the non-radiative decay rate is determined by the reciprocal of the average vibrational relaxation width $\langle\Gamma_l\rangle$ of the background states. We have just regenerated the original Robinson–Frosch formula[5], which is of limited utility.

10.13.2 Intermediate level structure

The statistical and the small-molecule limits represent well-defined, observable cases. Another potentially interesting situation involves the intermediate case when a small electronic energy gap exists between two electronic states of a large molecule[33,51]. It should be noted that now it is unjustified to use 'coarse graining' procedures employed in the statistical limit, which disregard the details of the variation of the interstate coupling terms and the level distribution in the background $\{|l\rangle\}$ manifold. These features have to be considered in detail for the intermediate case. The physical situation is closely related to the problem of intermediate structure in nuclear reactions[111,112], where the density of nuclear excitations is low and fine structure is exhibited in the nuclear scattering process.

As in the statistical and the small-molecule limits, we can consider a single resonance $|s,\text{vac}\rangle$ (see Figure 10.4). In view of simple symmetry arguments, not all the states in the $\{|l\rangle\}$ manifold are coupled to $|s\rangle$ with the same efficiency. When the total density of the former states is relatively low, for small electronic energy gaps, say 10^3–10^4 cm^{-1}, only few of these levels are effectively coupled to $|s\rangle$. We partition the $\{|l\rangle\}$ manifold into a small subset $\{|l_a\rangle\}$ of effectively coupled levels, and another subset $\{|l_b\rangle\}$ which contains the majority of the levels which are weakly coupled to $|s\rangle$. The

$\{|l_b\rangle\}$ manifold may be considered as a statistical dissipative channel which leads to irreversible intramolecular decay on the relevant time scale.

The state $|s,\text{vac}\rangle$ together with $|l_a,\text{vac}\rangle$ constitute a sparse manifold of discrete levels. The Hilbert subspace $\hat{P}$ spanned by the zero order states bears a close analogy to the small-molecule case, apart from the possibility of accidental degeneracies. It is convenient to find the molecular eigenstates $|n,\text{vac}\rangle$ which diagonalise $\hat{P}H_M\hat{P}$ while the effective Hamiltonian $\hat{P}(H_0 R)\hat{P}$ is

$$(H_{\text{eff}})_{nn'} = E_n\delta_{nn'} - (i/2)\,\gamma_{nn'} \tag{10.108}$$

while the decay matrix is given by

$$\gamma_{nn'} = \Gamma^{r}_{nn'} + \Gamma^{nr}_{nn'}$$

$$\Gamma^{r}_{nn'} = 2\pi\langle n,\text{vac}|H_{\text{int}}|g,ke\rangle\langle g,ke|H_{\text{int}}|n',\text{vac}\rangle\rho_r$$

$$\Gamma^{nr}_{nn'} = 2\pi\langle n,\text{vac}|H_t|l_b,\text{vac}\rangle\langle l_b,\text{vac}|H_r|n',\text{vac}\rangle\rho_{l_b} \tag{10.109}$$

The physical situation corresponds to a parallel decay of a discrete manifold $|n,\text{vac}\rangle$ into radiative and non-radiative continua.

Two cases of increasing complexity are considered:

(a) When the molecular eigenstates in $\hat{P}$ are well separated relative to their total widths, i.e. $\gamma_{nn'} \ll |E_n - E_{n'}|$ for all n and n', the situation is equivalent to that encountered in the small molecule case. The effective Hamiltonian is diagonal in the $|n,\text{vac}\rangle$ representation and the characteristic decay widths of the independently decaying levels are

$$\gamma_{nn} = |\langle s,\text{vac}|n,\text{vac}\rangle|^2(\Gamma^{r}_{s} + \Gamma^{nr}_{s}) \tag{10.110}$$

where the radiative width Γ^{r}_{s} and non-radiative widths Γ^{nr}_{s} of the doorway state are obtained from (10.109) by replacing both n and n' by s. The photon counting rate resulting from an excitation by a Lorentzian pulse is given by

$$I(t) \propto \sum_n \frac{\gamma_{nn}}{(E_n - \bar{k})^2 + (\gamma_p/2)^2}\exp(-\gamma_{nn}t) \tag{10.111}$$

which is analogous to (10.106) except that the radiative widths are replaced by the total widths γ_{nn}. As $|\langle s,\text{vac}|n,\text{vac}\rangle|^2 \ll 1$ for all n, then provided that $\Gamma^{nr}_{s} \sim \Gamma_s$ we expect that $\gamma_{nn} < \gamma_s$. The experimental decay width of the excited states $|n,\text{vac}\rangle$ now accessible by optical excitation is reduced relative to the radiative width of the zero-order state obtained from the integrated oscillator strength. We expect a lengthening of the radiative decay times of a large molecule which corresponds to the intermediate case[51].

(b) When some of the molecular eigenstates in $\hat{P}$ are closely spaced relative to their total widths, interference effects are exhibited in the radiative decay[51].

Consider some features of the intermediate case. We notice that the $\{|l_a\rangle\}$ manifold is non-dissipative, as the strong interstate coupling between $|s\rangle$ and $\{|l_a\rangle\}$ does not provide a pathway for electronic relaxation in the isolated molecule. One thus expects the lengthening of the radiative decay times relative to those estimated from the integrated oscillator strength. Thus a state of a large molecule which corresponds to the intermediate level structure exhibits the decay characteristics of the small-molecule case. This

theoretical prediction was experimentally confirmed for the S_2, S_1 coupling in 3,4-benzpyrene[167-170], naphthalene[171] and quinoxaline[173], and for the S_1-T_1 coupling in benzophenone[172] (see Table 10.8).

Table 10.8 Long radiative decay times of some excited electronic states of large molecules

Molecule	*Transition*	*Energy gap*/cm^{-1}	τ(exp)/sec	τ(integrated f)/s
3,4-Benzpyrene[170]	$S_2 \rightarrow S_0$	2800 (S_2–S_1)	7×10^{-8}	1×10^{-8}
Naphthalene[171]	$S_2 \rightarrow S_0$	3500 (S_2–S_1)	4×10^{-8}	1×10^{-8}
Benzophenone[172]	$S_1 \rightarrow S_0$	3000 (S_1–T_1)	1×10^{-3}	1×10^{-6}
Quinoxaline[173]	$S_2 \rightarrow S_0$	4100 $S_2(\pi\pi^*)$–$S_1(\pi^*n)$	4×10^{-3}	2×10^{-8}

The time-resolved decay mode in case (a) above may exhibit a superposition of exponential decays according to equation (10.111) and vary with the mean excitation energy (if the exciting pulse is sufficiently broad, i.e. $\gamma_p \gg \gamma_{nn}$). In case (b), quantum beats should be exhibited following excitation in a narrow energy range; however, this interesting effect may be smeared out owing to sequence congestion effects. Regarding medium effects, we note that when the molecule is perturbed by an external medium a new relaxation channel is added to the $|s\rangle$ state: $|s\rangle \rightarrow \{|l_a\rangle\} \rightarrow \{|l'_m\rangle\}$; consecutive relaxation occurs as collisions or phonon coupling provide a vibrational relaxation channel. To provide a verification of these conclusions we note that the S_1 state of the benzophenone molecule, which is separated by 2800 cm^{-1} from T_1 and which does not exhibit fluorescence in solution[148], exhibits fluorescence in the low-pressure gas phase[172].

10.14 PHOTON SCATTERING AND ABSORPTION CROSS SECTIONS

After exploring the nature of 'short excitation' experiments, we now consider the second extreme situation of a 'long time' excitation where one cannot separate the excitation and decay processes but rather consider photon scattering from large molecules as a single quantum mechanical process. No restrictions are imposed on the energy resolution of the photon field and we proceed to study the relevant cross sections (see Section 10.2) resulting from scattering of photons having energy $E = \hbar ck$.

Scattering theory provides a powerful tool for understanding the interaction of a molecular system with the radiation field which is responsible for the absorption lineshape and for photon scattering processes[75, 76, 80]. 'Long excitation' experimental observables pertaining to electronic relaxation

in large molecules can be handled[66,71] by considering a 'collision process' between a monochromatic wave train and the 'isolated' molecule within the framework of the Lippmann–Schwinger equation, expressed in terms of the T matrix formalism. The T matrix (the transition operator) is defined by

$$T = V + VG(E^+)V \tag{10.112}$$

where $E^+ = \lim_{\eta \to 0^+}(E + i\eta)$ and $V = H_V = H_{int}$. In the distant past, the molecule was in the continuum state $|a\rangle = |g0,ke\rangle$ characterised by the energy E_a. The final (continuum) states resulting from photon scattering are denoted by $|b\rangle = |gv,k_fe_f\rangle$ characterised by the energy E_b.

The cross section $\sigma(a \to b)$ for the transition $a \to b$ to a group of final states in the energy interval dE_b is obtained by dividing the transition probability by the photon flux $F = cQ$ where c is the velocity of light and Q represents the volume, and we use box normalisation for the radiation field. Thus the cross section is:

$$\sigma(a \to b) = (2\pi Q/\hbar c)|T_{ba}|^2\delta(E_b - E_a) \tag{10.113}$$

The second general result is the rate of disappearance, W_a, of the initial state $|a\rangle$, which is given by

$$W_a = -(2/\hbar)\, I_m(T_{aa}) \tag{10.114}$$

while the absorption cross section σ_a (at zero temperature) is given again by dividing by the flux

$$\sigma_a = -(2Q/\hbar c)\, I_m T_{aa} \tag{10.115}$$

We can immediately apply these results by setting for the initial energy $E_a = E(|g0,ke\rangle) = E_{v0} + E$ where E_{v0} is the energy of the ground vibrationless level and $E = khc$ is the incident photon energy, whereupon the absorption cross section is obtained from (10.115) in the form

$$\sigma_a(E) = -(2Q/hc)\, I_m\langle g0,ke|VG(E^+)V|g0,ke\rangle \tag{10.116}$$

Consider now the cross section for the photon-scattering process $|g0,ke\rangle \to |gv,k_fe_f\rangle$, which takes place between the initial state $|g0,ke\rangle$ characterised by the energy $E_{v0} + khc$ and the final states $|gv,k_fe_f\rangle$ characterised by the energy $E_{gv} + k_fhc$,

$$\sigma(g0,ke \to gv,k_fe_f) = 2\pi Q^2/\hbar c|\langle gv,k_fe_f|T|g0,ke\rangle|^2\rho_v(k_f) \tag{10.117}$$

The photon scattering cross section $\sigma_r^v(E)$ into the final molecular state $|gv\rangle$ is obtained by summing (10.117) over all final spatial directions and polarisation directions:

$$\sigma_r^v(E) = \langle \sum_{e_f} \int d\Omega_{k_f}\sigma(g0,ke \to gv,k_fe_f) \tag{10.118}$$

where $\langle\ \rangle$ denotes averaging over initial molecular orientations with respect to the photon polarisation. The total cross section for resonance fluorescence

theoretical prediction was experimentally confirmed for the S_2-S_1 coupling in 3,4-benzpyrene[167-170], naphthalene[171] and quinoxaline[173], and for the S_1-T_1 coupling in benzophenone[172] (see Table 10.8).

Table 10.8 Long radiative decay times of some excited electronic states of large molecules

Molecule	*Transition*	*Energy gap*/cm^{-1}	τ(exp)/sec	τ(integrated f)/s
3,4-Benzpyrene[170]	$S_2 \rightarrow S_0$	2800 (S_2–S_1)	7×10^{-8}	1×10^{-8}
Naphthalene[171]	$S_2 \rightarrow S_0$	3500 (S_2–S_1)	4×10^{-8}	1×10^{-8}
Benzophenone[172]	$S_1 \rightarrow S_0$	3000 (S_1–T_1)	1×10^{-3}	1×10^{-6}
Quinoxaline[173]	$S_2 \rightarrow S_0$	4100 $S_2(\pi\pi^*)$–$S_1(\pi^*n)$	4×10^{-3}	2×10^{-8}

The time-resolved decay mode in case (a) above may exhibit a superposition of exponential decays according to equation (10.111) and vary with the mean excitation energy (if the exciting pulse is sufficiently broad, i.e. $\gamma_p \gg \gamma_{nn}$). In case (b), quantum beats should be exhibited following excitation in a narrow energy range; however, this interesting effect may be smeared out owing to sequence congestion effects. Regarding medium effects, we note that when the molecule is perturbed by an external medium a new relaxation channel is added to the $|s\rangle$ state: $|s\rangle \rightarrow \{|l_n\rangle\} \rightarrow \{|l'_m\rangle\}$; consecutive relaxation occurs as collisions or phonon coupling provide a vibrational relaxation channel. To provide a verification of these conclusions we note that the S_1 state of the benzophenone molecule, which is separated by 2800 cm^{-1} from T_1 and which does not exhibit fluorescence in solution[148], exhibits fluorescence in the low-pressure gas phase[172].

10.14 PHOTON SCATTERING AND ABSORPTION CROSS SECTIONS

After exploring the nature of 'short excitation' experiments, we now consider the second extreme situation of a 'long time' excitation where one cannot separate the excitation and decay processes but rather consider photon scattering from large molecules as a single quantum mechanical process. No restrictions are imposed on the energy resolution of the photon field and we proceed to study the relevant cross sections (see Section 10.2) resulting from scattering of photons having energy $E = \hbar ck$.

Scattering theory provides a powerful tool for understanding the interaction of a molecular system with the radiation field which is responsible for the absorption lineshape and for photon scattering processes[75, 76, 80]. 'Long excitation' experimental observables pertaining to electronic relaxation

in large molecules can be handled[66,71] by considering a 'collision process' between a monochromatic wave train and the 'isolated' molecule within the framework of the Lippmann–Schwinger equation, expressed in terms of the T matrix formalism. The T matrix (the transition operator) is defined by

$$T = V + VG(E^+)V \tag{10.112}$$

where $E^+ = \lim_{\eta \to 0^+}(E + i\eta)$ and $V = H_V + H_{int}$. In the distant past, the molecule was in the continuum state $|a\rangle = |g0,ke\rangle$ characterised by the energy E_a. The final (continuum) states resulting from photon scattering are denoted by $|b\rangle = |gv,k_f e_f\rangle$ characterised by the energy E_b.

The cross section $\sigma(a \to b)$ for the transition $a \to b$ to a group of final states in the energy interval dE_b is obtained by dividing the transition probability by the photon flux $F = cQ$ where c is the velocity of light and Q represents the volume, and we use box normalisation for the radiation field. Thus the cross section is:

$$\sigma(a \to b) = (2\pi Q/\hbar c)|T_{ba}|^2 \delta(E_b - E_a) \tag{10.113}$$

The second general result is the rate of disappearance, W_a, of the initial state $|a\rangle$, which is given by

$$W_a = -(2/\hbar)\, I_m(T_{aa}) \tag{10.114}$$

while the absorption cross section σ_a (at zero temperature) is given again by dividing by the flux

$$\sigma_a = -(2Q/\hbar c)\, I_m T_{aa} \tag{10.115}$$

We can immediately apply these results by setting for the initial energy $E_a = E(|g0,ke\rangle) = E_{v0} + E$ where E_{v0} is the energy of the ground vibrationless level and $E = khc$ is the incident photon energy, whereupon the absorption cross section is obtained from (10.115) in the form

$$\sigma_a(E) = -(2Q/hc)\, I_m\langle g0,ke|VG(E^+)V|g0,ke\rangle \tag{10.116}$$

Consider now the cross section for the photon-scattering process $|g0,ke\rangle \to |gv,k_f e_f\rangle$, which takes place between the initial state $|g0,ke\rangle$ characterised by the energy $E_{v0} + khc$ and the final states $|gv,k_f e_f\rangle$ characterised by the energy $E_{gv} + k_f hc$,

$$\sigma(g0,ke \to gv,k_f e_f) = 2\pi Q/\hbar c|\langle gv,k_f e_f|T|g0,ke\rangle|^2 \rho_r(k_f) \tag{10.117}$$

The photon scattering cross section $\sigma_r^v(E)$ into the final molecular state $|gv\rangle$ is obtained by summing (10.117) over all final spatial directions and polarisation directions:

$$\sigma_r^v(E) = \left\langle \sum_{e_f} \int d\Omega_{k_f} \sigma(g0,ke \to gv,k_f e_f) \right\rangle \tag{10.118}$$

where $\langle\ \rangle$ denotes averaging over initial molecular orientations with respect to the photon polarisation. The total cross section for resonance fluorescence

is obtained by monitoring all the emitted photons resulting from scattering into all the final molecular states $|g\rangle$.

$$\sigma_r(E) = \sum_{\nu} \sigma_r^{\nu}(E) \tag{10.119}$$

In a similar manner we can define a cross section $\sigma_{nr}(E)$ for effective scattering into the quasi-continuum $\{|I,\text{vac}\rangle\}$, which we consider to be an operational continuum. This is given by

$$\sigma_{nr}(E) = (2\pi Q/\hbar c)|\langle g0,ke|T(E)|I,\text{vac}\rangle|^2 \rho_I(E) \tag{10.120}$$

The unitarity relations for the scattering matrix result in the optical theorem of scattering theory[80]

$$-(1/\pi)\, I_m T_{aa} = \sum_{\text{all } b} |T_{ba}|^2 \delta(E_a - E_b) \tag{10.121}$$

which leads to the conservation law

$$\sigma_a(E) = \sum_{\nu} \sigma_R^{\nu}(E) + \sigma_{nr}(E) \tag{10.122}$$

The (energy dependent) quantum yield resulting from absorption of a photon of energy E leading to the molecular state $|g\nu\rangle$ is given by the ratio of the resonance scattering cross section, equation (10.118), and the absorption cross section, equation (10.116), $Y_\nu(E) = \sigma_r^\nu(E)/\sigma_a(E)$. If the ground state energy levels are well spaced, the different channels can be resolved. Finally, the total quantum yield for emission is given by $Y(E) = \sum_{\nu} Y_\nu(E) = \sigma_r(E)/\sigma_a(E)$. In a similar way the quantum yield for electronic relaxation in a statistical molecule (or for predissociation) is $Y_{nr}(E) = \sigma_{nr}(E)/\sigma_a(E)$ and (10.122) implies that $Y(E) + Y_{nr}(E) = 1$. The general expression for the absorption cross sections, for the resonance fluorescence cross sections and for the emission quantum yields in the 'statistical' molecular case will involve as 'open channels' not only the radiation continuum but also the intramolecular quasi-continuum $\{|I,\rangle\}$, which for all practical purposes can be considered as an 'open' decay channel. In this case the unitarity relations for the scattering matrix do not imply that $Y(E)$ is equal to unity as intramolecular decay channels have to be considered.

Let us now establish the relation between the relevant cross sections and the independently decaying discrete molecular states discussed in Section 10.10. As we are interested in parallel coupling of the discrete levels $|m,\text{vac}\rangle$ to radiative and non-radiative channels we shall consider the effective Hamiltonian H_{eff}, equation (10.83), characterised by the eigenstates $|J,\text{vac}\rangle$. Apart from irrelevant numerical factors, the cross sections are

$$\sigma_r^{\nu}(E) \propto \Big|\sum_J \frac{\langle g\nu,k_f e_f|H_{\text{int}}|J,\text{vac}\rangle\langle J,\text{vac}|H_{\text{int}}|g0,ke\rangle}{E - E_J + i\gamma_J/2}\Big|^2 \rho_r(k_f)$$

$$\sigma_a(E) \propto \sum_J I_m \frac{\langle g0,ke|H_{\text{int}}|J,\text{vac}\rangle\langle J,\text{vac}|H_{\text{int}}|g0,ke\rangle}{E - E_J + i\gamma_J/2} \tag{10.123}$$

where γ_J represents the total (radiative plus non-radiative) widths of the independently decaying states. These results exhibit some interesting features.

The photon-scattering cross section $\sigma_r(E)$ definitely involve interference effects provided that $|E_j - E_i| \lesssim \gamma_j, \gamma_i$. This is the analogue of the quantum beats expected under these circumstances for short-time excitation experiments. The expression for the absorption cross section reveals formally a superposition of Lorentzians. This feature should not mislead the uninitiated reader, as one has to bear in mind that the states $|J,\text{vac}\rangle$ and their complementary states $|\bar{J},\text{vac}\rangle$ are characterised by complex expansion coefficients of $|m,\text{vac}\rangle$, whereupon the single sum (10.123) exhibits interference effects of the absorption lineshape for closely spaced (relative to γ_j) levels.

Several illustrative cases should be now briefly considered. In the simplest physical situation of a single resonance, the manifold $\{|J,\text{vac}\rangle, |\bar{J},\text{vac}\rangle\}$ contains a single level $|s,\text{vac}\rangle$, whereupon σ_r^e and $\sigma_a(E) \propto [(E - E_s)^2 + (\gamma_s/2)^2]^{-1}$, all cross sections exhibiting a Lorentzian energy dependence. For the more interesting case of interference between a small number of closely spaced discrete levels, interference effects in the cross section are exhibited. From model calculations[66] for interference between a pair of resonances (see Figure 10.13) one concludes that (i) depending on the relative displacement of potential surfaces (expressed in terms of the reduced displacement Δ) destructive interference is exhibited in $\sigma_a(E)$ and in $\sigma_r^e(E)$ either outside or inside the energy region between the two resonances, (ii) when radiative interactions are incorporated to infinite order, $\sigma_a(E)$ does not vanish but assumes a very low value in the region of destructive interference, (iii) in the vicinity of the interference dip in $\sigma_a(E)$ both the partial and total quantum yields for photon scattering exhibit a sharp maximum. The destructive interference effect does not result in $\sigma_a = 0$ at the dip but rather implies the vanishing of the cross section for scattering into the intramolecular non-radiative channel.

We have recently established[71] the relation between the theoretical treatment of the time evolution of the molecular system resulting from wave packet excitation in 'short time' excitation experiments and the study of photon scattering cross sections involved in 'long time' excitation conditions. This was accomplished by pursuing the general relations between the reaction matrix T and the (photon) scattering matrix S. This formalism results in general useful results for the quantum yields expressed in terms of the pulse amplitudes $A_k = A(E)$, and the relevant cross sections [71]

$$Y_v = \frac{\int |A(E)|^2 \sigma_r^e(E) \mathrm{d}E}{\int |A(E)|^2 \sigma_a(E) \mathrm{d}E} \tag{10.124}$$

$$Y_{nr} = \frac{\int |A(E)|^2 \sigma_{nr}(E) \mathrm{d}E}{\int |A(E)|^2 \sigma_a(E) \mathrm{d}E} \tag{10.125}$$

These results are valid for all excitation conditions. We note that in general the quantum yields are determined by the power spectrum of the source, and the only relevant information required concerning the excitation source involves its energetic spread and not the phases of the radiation field. In the 'long time' excitation limit $|A(E)|^2$ is sharply peaked around E and the quantum yields are given in terms of the ratios of the cross sections at this particular energy. In the extreme case of short excitation conditions $|A(E)|^2$ is a slowly

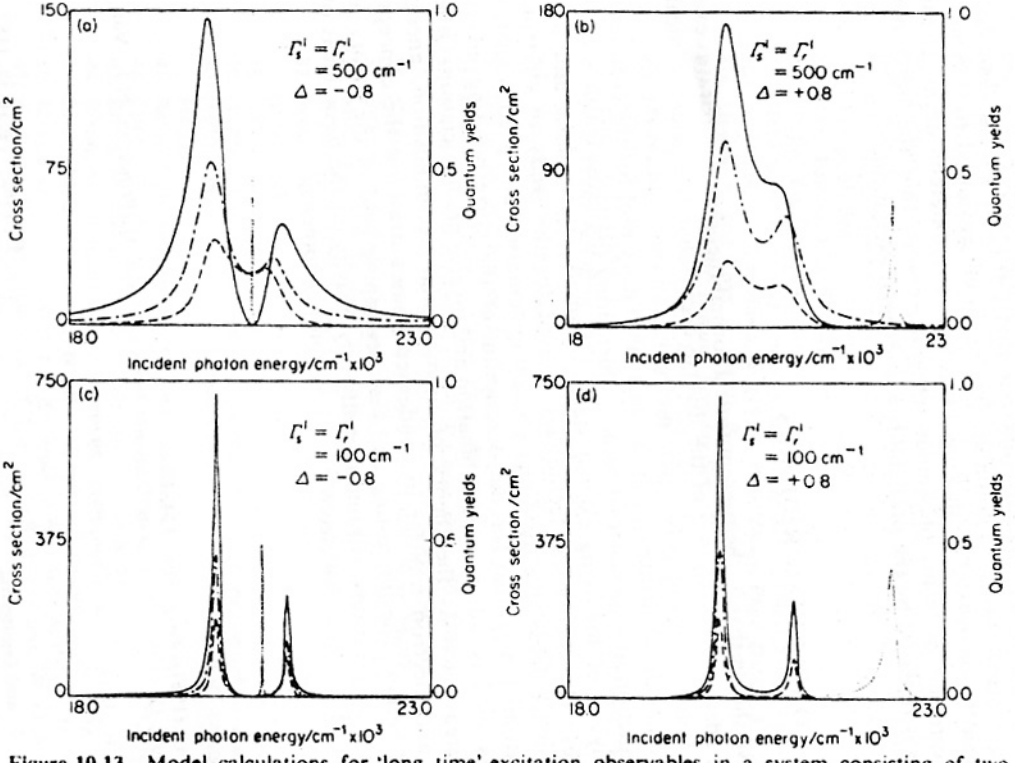

Figure 10.13 Model calculations for 'long time' excitation observables in a system consisting of two decaying resonances s and r. The electronic energy gap is taken to be 20 000 cm^{-1} and the optically active frequency is 1000 cm^{-1}. The radiative widths are governed by the Franck–Condon factors which in turn are determined by the origin displacement Δ between the ground and excited electronic states. The non-radiative widths are 500 or 100 cm^{-1} for both s and r. ——, absorption cross section; — — —, partial emission cross section to $v = 1$; —·—·—, total emission cross section; - - -, partial quantum yield; . . ., total quantum yield. The cross sections are given in relative units, while the absolute values for quantum yields are displayed

varying function of the energy and the quantum yields reduce to the ratio of the integrals over the cross sections. In these two limits the quantum yields are solely determined by the molecular parameters and not by the characteristics of the source. In general, the quantum yields are different under different excitation conditions. Only when both cross sections $\sigma_r(E)$ and $\sigma_d(E)$ exhibit the same energy dependence Y_i will be independent on the pulse characteristics under all excitation conditions. This situation is encountered only in the special, but useful, case of a single molecular resonance, when both cross sections exhibit a Lorentzian energy dependence.

Finally, we would like to point out that (10.125) bears a close formal analogy to the theory of unimolecular reactions advanced by Levine and Coulson[174], where the branching ratio between different decay channels are expressed in terms of similar integrals, except that the pulse power system is replaced by the probability for thermal excitation.

10.15 CONCLUDING REMARKS

We have shown that at the present time a formal theoretical apparatus exists for the adequate description of the diverse decay channels of electronically excited bound states of polyatomic molecules. In our opinion the theory in this field has demonstrated its utility as a laboratory tool for the correlation and prediction of experimental results, elucidating the gross features of the photophysics of low-lying excited states of small, intermediate and large molecules. The theoretical techniques utilised for the study of electronic relaxation are applicable for direct photofragmentation and predissociation of polyatomics and also for the description of the corresponding inverse processes, such as radiative recombination and inverse predissociation. Other related areas such as the theory of unimolecular decomposition, energy transfer and electron transfer in condensed phases draw on the concepts discussed herein. The interesting and fast developing field of the theory of photochemical reactions will undoubtedly rely heavily on the basic ideas of the theory of non-reactive electronic relaxation phenomena.

References

1. Fano, U. (1961). *Phys. Rev.*, **124**, 1866
2. Herzberg, G. (1954). *Spectra of Diatomic Molecules*, Vol. II (Princeton, N.J.: Van Nostrand)
3. Harris, R. A. (1963). *J. Chem. Phys.*, **39**, 978

4a. Kasha, M. (1960). *Discuss. Faraday Soc.*, No. 9, 14

4b. Kasha, M. (1960). *Radiation Res. Suppl.*, **2**, 243

5. Robinson, G. W. and Frosch, R. P. (1962). *J. Chem. Phys.*, **37**, 1962; (1963). **38**, 1187
6. Seybold, P. and Gouterman, M. (1965). *Chem. Rev.*, **65**, 413
7. Lower, S. K. and El-Sayed, M. A. (1966). *Chem. Rev.*, **66**, 199
8. Henry, B. R. and Kasha, M. (1968). *Ann. Rev. Phys. Chem.*, **19**, 161
9. Jortner, J., Rice, S. A. and Hochstrasser, R. W. (1969). In *Advan. Photochemistry*, Vol. 7 (W. A. Noyes, J. N. Pitts and G. Hammond, editors) (New York: Wiley)
10. Jortner, J. (1970). *Pure Appl. Chem.*, **24**, 165

11. Jortner, J. (1970). *J. Chim. Phys.*, special issue No. 20, *Transitions non-radiatives dans les molecules*, p. 1
12. Bixon, M. and Jortner, J. (1968). *Israel J. Chem.*, **48**, 715
13. Jortner, J. (1971). In *Organic Solid State Chemistry*, Vol. 2 (M. D. Cohen, editor) (London: Butterworths)
14. Schlag, E. W., Schneider, S. and Fischer, S. F. (1971). *Ann. Rev. Phys. Chem.*, **22**, 465
15. Freed, K. F. (1972). *Topics Current Chem.*, **31**, 105
16. Henry, B. R. and Siebrand, W., to be published
17a. Montroll, E. W. and Shuler, K. E. (1957). *J. Chem. Phys.*, **26**, 454
17b. Nitzan, A. and Jortner, J. (1973). *Mol. Phys.*, **25**, 713
18a. Gilbert, R. G. and Ross, I. G. (1971). *Aust. J. Chem.*, **24**, 1541
18b. Gebelein, H. and Jortner, J. (1972). *Theor. Chim. Acta*, **25**, 487
19. Turro, N. (1965). *Molecular Photochemistry* (New York: Benjamin); Calvert, J. and Pitts, J. N. (1966). *Photochemistry* (New York: Wiley)
20a. Gelbart, W. M. and Rice, S. A. (1969). *J. Chem. Phys.*, **50**, 4775
20b. Gelbart, W. M., Freed, K. F. and Rice, S. A. (1970). *J. Chem. Phys.*, **52**, 2460
21. Rice, S. A. *Some Comments on the Dynamics of Primary Photochemical Processes*, to be published
22a. Markham, J. J. (1959). *Rev. Mod. Phys.*, **31**, 956
22b. Perlin, Yu. E. (1964). *Sov. Phys. Usp.*, **6**, 542
22c. Rebane, K. K. (1970). *Impurity Spectra of Solids*, (New York: Plenum Press)
22d. Kubo, R. and Toyozawa, Y. (1955). *Proc. Theor. Phys. Osaka*, **13**, 161
22e. Huang, K. and Rhys, A. (1950). *Proc. Roy Soc.*, **A204**, 406
23. Förster, Th. (1959). *Discuss. Faraday Soc.*, No. 27, 7
24. Dexter, D. L. (1953). *J. Chem. Phys.*, **21**, 836
25. Soules, T. F. and Duke, C. B. (1971). *Phys. Rev.*, **B3**, 262
26. Jortner, J. (1968). *Phys. Rev. Lett.*, **20**, 244
27. Levich, V. G. (1970). In *Physical Chemistry—An Advanced Treatise* (H. Eyring, editor) (New York: Academic Press)
28a. Jortner, J. (1971). *Ber. Bunsenges. Phys. Chem.*, **75**, 697
28b. Rentzepis, P. M., Jones, R. P. and Jortner, J. (1973). *J. Chem. Phys.*, **59**, 766
29. Robinson, G. W. (1967). *J. Chem. Phys.*, **47**, 1967
30. Bixon, M. and Jortner, J. (1968). *J. Chem. Phys.*, **48**, 715
31. Rhodes, W. (1969). *J. Chem. Phys.*, **50**, 2885
32. Bixon, M. and Jortner, J. (1969). *J. Chem. Phys.*, **50**, 3284
33. Freed, K. F. and Jortner, J. (1969). *J. Chem. Phys.*, **50**, 2916
34. Nitzan, A. and Jortner, J. (1973). *Theor. Chim. Acta*, **29**, 97
35. Birks, J. B. (1970). *Photophysics of Aromatic Molecules* (New York: Wiley)
36. McGlynn, S. P., Azumi, T. and Kinoshita, M. (1969). *Molecular Spectroscopy of the Triplet State*, (Englewood Cliffs, N.J.: Prentice Hall)
37. Becker, R. S. (1969). *Theory and Interpretation of Fluorescence and Phosphorescence*, (New York: Wiley)
38. (1969). *Molecular Luminescence*, (E. D. Lim, editor) (New York: Benjamin)
39. (1970). *J. Chim. Phys.*, special issue No. 20, *Transitions non radiatives dans les molécules*
40. (1970). *Proc. Int. Conf. Luminescence*, (F. Williams, editor) (Amsterdam: North Holland)
41. Berry, R. S. and Jortner, J. (1968). *J. Chem. Phys.*, **48**, 2757
42. Chock, D., Rice, S. A. and Jortner, J. (1968). *J. Chem. Phys.*, **49**, 610
43. Bixon, M. and Jortner, J. (1969). *Mol. Crystals*, **213**, 237
44. Bixon, M., Dothan, Y. and Jortner, J. (1969). *Mol. Phys.*, **17**, 109
45. Bixon, M. and Jortner, J. (1969). *J. Chem. Phys.*, **50**, 4061
46. Morris, G. C. and Jortner, J. (1969). *J. Chem. Phys.*, **51**, 3689
47. Englman, R. and Jortner, J. (1970). *Mol. Phys.*, **18**, 145
48. Freed, K. F. and Jortner, J. (1970). *J. Chem. Phys.*, **52**, 6272
49. Gelbart, W. M., Spears, K. G., Freed, K. F., Rice, S. A. and Jortner, J. (1970). *Chem. Phys. Lett.*, **6**, 345
50. Gelbart, W. M. and Jortner, J. (1971). *J. Chem. Phys.*, **54**, 2070
51. Nitzan, A., Rentzepis, P. M. and Jortner, J. (1972). *Proc. Roy. Soc.*, **A327**, 367
52. Jortner, J. (1971). *J. Chem. Phys.*, **55**, 1355
53. Nitzan, A., Rentzepis, P. M. and Jortner, J. (1971). *Chem. Phys. Lett.*, **8**, 445

54. Nitzan, A., Kommandeur, J., Drent, E. and Jortner, J. (1971). *Chem. Phys. Lett.*, **9**, 273
55. Nitzan, A., Rentzepis, P. M. and Jortner, J. (1972). *Mol. Phys.*, **22**, 585
56. Jortner, J. (1971). *Chem. Phys. Lett.*, **11**, 458
57. Nitzan, A. and Jortner, J. (1972). *J. Chem. Phys.*, **56**, 3360
58. Nitzan, A. and Jortner, J. (1972). *J. Chem. Phys.*, **56**, 2079
59. Nitzan, A. and Jortner, J. (1971). *J. Chem. Phys.*, **55**, 1305
60. Jortner, J. (1972). *J. Chem. Phys.*, **56**, 5742
61. Nitzan, A. and Jortner, J. (1972). *J. Chem. Phys.*, **56**, 5200
62. Nitzan, A. and Jortner, J. (1972). *Chem. Phys. Lett.*, **13**, 466
63. Nitzan, A. and Jortner, J. (1972). *Mol. Phys.*, **24**, 109
64. Nitzan, A. and Jortner, J. (1972). *Chem. Phys. Lett.*, **14**, 177
65a. Nitzan, A. and Jortner, J. (1973). *J. Chem. Phys.*, **58**, 2412
65b. Nitzan, A. and Jortner, J. (1972). *Chem. Phys. Lett.*, **15**, 350
66. Nitzan, A. and Jortner, J. (1972). *J. Chem. Phys.*, **57**, 2870
67. Nitzan, A. and Jortner, J. (1973). *Mol. Phys.*, **25**, 713
68. Nitzan, A. and Jortner, J. (1973). *Theor. Chim. Acta*, **30**, 217
69. Nitzan, A. and Jortner, J. (1973). *J. Chem. Phys.*, **58**, 2669
70. Nitzan, A., Berne, B. J. and Jortner, J. (1973). *Mol. Phys.*, **26**, 281
71. Jortner, J. and Mukamel, S. (1974). In *The World of Quantum Chemistry* (R. Daudel and B. Pullman, editors) (D. Reidel)
72. Mukamel, S. and Jortner, J. (1974). *J. Chem. Phys.*, **61**, 227, 436
73. Mukamel, S. and Jortner, J. (1974). *J. Chem. Phys.*, **60**, 4760
74. Mukamel, S. and Jortner, J. (1974). *Mol. Phys.*, **27**, 1543
75. Goldberger, M. L. and Watson, R. M. (1969). *Collision Theory* (New York: Wiley)
76. Cohen-Tannoudi, C. (1968). In *Introduction a l'electronique quantique cours de l' Association Vandoire des chercheres en physique*, (Saas Fee)
77. Rhodes, W., Henry, B. R. and Kasha, M. (1969). *Proc. Nat. Acad. Sci. USA*, **63**, 31
78. Freed, K. F. (1970). *J. Chem. Phys.*, **52**, 1345
79. Rhodes, W. (1971). *Chem. Phys. Lett.*, **11**, 179
80. Shore, B. W. (1967). *Rev. Mod. Phys.*, **39**, 439
81. Franck, J. and Sponer, H. (1928). *Göttingen Nachricht*, 241
82. Kubo, R. (1952). *Phys. Rev.*, **86**, 929
83. Born, M. and Huang, K. (1956). *Dynamical Theory of Crystal Lattices*, (Oxford: University Press)
84. Longuet-Higgins, H. C. (1961). *Advan. Spectrosc.*, **2**, 429
85. Englman, R. (1972). *The Jahn-Teller Effect in Molecules and Crystals*, (New York: Wiley)
86. Herzberg, G. and Teller, E. (1933). *Z. Phys. Chem.*, **B21**, 410
87. Sharf, B. and Silbey, R. (1969). *Chem. Phys. Lett.*, **4**, 423
88. Sharf, B. and Silbey, R. (1970). *Chem. Phys. Lett.*, **4**, 561
89. Burland, D. M. and Robinson, G. W. (1970). *Proc. Nat. Acad. Sci. USA*, **66**, 257
90. Sharf, B. (1971). *Chem. Phys. Lett.*, **6**, 364; (1971). *ibid.*, **8**, 238, 391
91. Sharf, B. and Silbey, R. (1971). *Chem. Phys. Lett.*, **9**, 125
92. Orlandi, G. and Siebrand, W. (1971). *Chem. Phys. Lett.*, **8**, 473
93. Siebrand, W. (1971). *Chem. Phys. Lett.*, **9**, 157
94. Freed, K. F. and Gelbart, W. M. (1971). *Chem. Phys. Lett.*, **10**, 187
95. Lefebvre, R. (1971). *Chem. Phys. Lett.*, **8**, 306
96. Atabek, O., Hardisson, A. and Lefebvre, R. (1973). *Chem. Phys. Lett.*, **20**, 40
97. Lefebvre, R. and Beswick, J. A. (1972). *Mol. Phys.*, **23**, 1223
98. Hobey, W. D. and McLachlan, A. D. (1960). *J. Chem. Phys.*, **33**, 1695
99. Lin, S. H. and Bersohn, R. (1968). *J. Chem. Phys.*, **32**, 1261
100a. Kovarskii, V. A. (1963). *Soviet Phys. Solid State*, **4**, 1200
100b. Kovarskii, V. A. and Sinyavskii, E. P. (1961). *Soviet Phys. Solid State*, **4**, 2435
101. Child, M. S. (1974). *Diatomic Predissociation Line Widths*. In *Specialist Periodical Report on Molecular Spectroscopy*, Vol. 2 (R. F. Barrow, editor) (London: Chemical Society)
102. Pople, J. A. and Sidman, J. W. (1957). *J. Chem. Phys.*, **27**, 1270
103a. Siebrand, W. (1970). *Chem. Phys. Lett.*, **6**, 192
103b. Lawetz, V., Orlandi, G. and Siebrand, W. (1972). *J. Chem. Phys.*, **56**, 4058
103c. Henry, B. R. and Siebrand, W. (1969). *J. Chem. Phys.*, **51**, 2396

104. Burland, D. H. and Robinson, G. W. (1969). *J. Chem. Phys.*, **51**, 4548
105a. Christie, J. R. and Craig, D. P. (1972). *Mol. Phys.*, **23**, 353
105b. Metz, F., Friedrich, S. and Holnetcher, G. (1972). *Chem. Phys. Lett.*, **16**, 353
106. Slanger, T. G. and Black, G. (1973). *J. Chem. Phys.*, **58**, 194
107. Czarny, J., Felenbok, P. and Lefebvre, B. H. (1971). *J. Phys.*, **B4**, 124
108. Kovacs, I. (1969). *Rotational Structure in the Spectra of Diatomic Molecules*, (New York: American Elsevier)
109. Parmenter, C. S. and Schuh, M. D. (1972). *Chem. Phys. Lett.*, **13**, 120
110. Hunter, T. F. and Stock, M. G. (1973). *Chem. Phys. Lett.*, **22**, 371
111. Feshbach, H. (1958). *Ann. Phys. New York*, **5**, 357; (1967). *ibid.*, **43**, 410; Estrada, L. and Feshbach, H. (1963). *Ann. Phys. New York*, **23**, 123
112. Feshbach, H., Kerman, A. K. and Lemmer, R. H. (1967). *Ann. Phys. New York*, **41**, 230
113. Douglas, A. E. (1966). *J. Chem. Phys.*, **45**, 1007
114a. Mower, L. (1966). *Phys. Rev.*, **142**, 799
114b. Mower, L. (1968). *Phys. Rev.*, **165**, 145
115. Ben-Reuven, A. (1974). *Advan. Chem. Phys.*, in press
116. Haken, H. (1970). *Handbuch der Physik*, Vol. XXV/2C, (Springer Verlag)
117. Schweber, S. S. (1961). *An Introduction to Relativistic Quantum Field Theory*, (New York: Row, Peterson)
118a. Glauber, R. J. (1963). *Phys. Rev.*, **131**, 2766
118b. (1965). *Quantum Optics and Electronics*, (C. DeWitt *et al.*, editors) (New York: Les Houches)
118c. (1969). *Quantum Optics, Proc. Int. School of Physics, Enrico Fermi Course XLII* (R. J. Glauber, editor) (London: Academic Press)
119. Mukamel, S. and Jortner, J. (1974). *J. Chem. Phys.*, in press
120. Williams, P. F., Rousseau, D. L. and Dworetsky, S. H. (1974). *Phys. Rev. Lett.*, **32**, 196
121. Weisskopf, V. F. and Wigner, E. P. (1930). *Z. Phys.*, **63**, 54; *ibid.*, **65**, 18
122. Siebrand, W. (1972). *Chem. Phys. Lett.*, **14**, 23
123. Drent, E. and Kommandeur, J. (1971). *Chem. Phys. Lett.*, **8**, 303
124. Kay, K. G. and Rice, S. A. (1972). *J. Chem. Phys.*, **57**, 3041
125. Lefebvre, R. and Beswick, J. A. (1972). *Mol. Phys.*, **23**, 1223
126a. Lahnani, F., Tramer, A. and Tric, C. M. (1974). *J. Chem. Phys.*, **60**, 4431
126b. Tric, C. M. (1974). *Chem. Phys.*, in press
127a. Watts, R. J. and Strickler, S. J. (1966). *J. Chem. Phys.*, **44**, 2423
127b. Williams, R. and Goldsmith, G. J. (1963). *J. Chem. Phys.*, **39**, 2008
128. Ware, W. R. and Cunningham, P. T. (1966). *J. Chem. Phys.*, **44**, 4364
129. Kistiakowski, G. B. and Parmenter, C. S. (1965). *J. Chem. Phys.*, **42**, 2942
130. Anderson, E. M. and Kistiakowski, G. B. (1968). *J. Chem. Phys.*, **48**, 4787
131. Douglas, A. E. and Mathews, C. W. (1968). *J. Chem. Phys.*, **48**, 4788
132. Huppert, D., Jortner, J. and Rentzepis, P. M. (1972). *J. Chem. Phys.*, **56**, 4826
133. Fischer, S. and Schneider, S. (1971). *Chem. Phys. Lett.*, **10**, 392
134. Brailsford, A. D. and Chang, Y. T. (1970). *J. Chem. Phys.*, **53**, 3108
135. Fisher, S. F. and Schlag, E. W. (1969). *Chem. Phys. Lett.*, **4**, 393
136. Fisher, S. F. (1969). *Chem. Phys. Lett.*, **4**, 333
137. Siebrand, W. (1972). *J. Chem. Phys.*, **55**, 1355
138a. Heller, D. F. and Freed, K. F. (1972). *Int. J. Quantum Chem.*, **6**, 267
138b. Heller, D. F., Freed, K. F. and Gelbart, W. M. (1972). *J. Chem. Phys.*, **56**, 2309; (1973). *Chem. Phys. Lett.*, in press
139. Lim, E. C. and Huang, C. S. (1973). *J. Chem. Phys.*, **58**, 1247
140. Selinger, B. K. and Ware, W. R. (1970). *J. Chem. Phys.*, **52**, 5482; (1970). *ibid.*, **53**, 3160
141. Parmenter, C. S. and Schuyler, M. W. (1970). *J. Chem. Phys.*, **52**, 5366; (1970). *Chem. Phys. Lett.*, **6**, 339
142. Ware, W. R., Selinger, B. K., Parmenter, C. S. and Schuyler, M. W. (1970). *Chem. Phys. Lett.*, **6**, 342
143. Schlag, E. W. and Weyssenhoff, H. V. (1969). *J. Chem. Phys.*, **51**, 2508
144a. Spears, K. G. and Rice, S. A. (1971). *J. Chem. Phys.*, **55**, 5561
144b. Abramson, A. S., Spears, K. G. and Rice, S. A. (1972). *J. Chem. Phys.*, **56**, 2291
144c. Guttman, C. and Rice, S. A. to be published
145. Weyssenhoff, H. V. and Kraus, F. (1971). *J. Chem. Phys.*, **54**, 2387

146a. Laor, U. and Ludwig, P. K. (1971). *J. Chem. Phys.*, **57**, 1054
146b. Uy, J. O. and Lim, E. C. (1970). *Chem. Phys., Lett.*, **7**, 306
146c. Hsieh, J. C., Laor, U. and Ludwig, P. K. (1971). *Chem. Phys. Lett.*, **10**, 412
147. Rockly, M. G. and Phillips, D. (1973). *Chem. Phys. Lett.*, **21**, 181
148a. Rentzepis, P. M. (1970). *Science*, **169**, 239
148b. Rentzepis, P. M. (1974). *Advan. Chem. Phys.*, in press
149a. Fischer, S., Schlag, E. W. and Schneider, S. (1971). *Chem. Phys. Lett.*, **11**, 583
149b. Fischer, S. (1972). *Chem. Phys. Lett.*, **17**, 25
150. Fischer, S. (1972). *J. Chem. Phys.*, **56**, 5199
151. Atkinson, R. B. and Thrush, B. A. (1970). *Proc. Roy. Soc.*, **A316**, 123, 131, 143
152. Yeung, E. S. and Moore, C. B. (1973). *J. Chem. Phys.*, **58**, 3988
153. Callomon, J. H., Lopez-Delgado, R. and Parkin, J. E. (1972). *Chem. Phys. Lett.*, **13**, 125
154a. Hemminger, J. C. and Lee, E. K. C. (1972). *J. Chem. Phys.*, **56**, 5284
154b. Hemminger, J. C., Rusbult, C. R. and Lee, E. K. C. (1971). *J. Amer. Chem. Soc.*, **93**, 1867
155. Lin, S. H. (1966). *J. Chem. Phys.*, **44**, 3759
156a. Hutchison, C. A. Jr. and Magnum, B. W. (1960). *J. Chem. Phys.*, **32**, 1261
156b. Wright, M. R., Frosch, R. P. and Robinson, G. W. (1960). *J. Chem. Phys.*, **33**, 934
156c. de Groot, M. S. and van der Waals, J. H. (1961). *Mol. Phys.*, **4**, 189
156d. Len, E. C. and Laposa, J. D. (1964). *J. Chem. Phys.*, **41**, 3257
156e. Kellogg, R. E. and Wyeth, N. C. (1966). *J. Chem. Phys.*, **45**, 3156
156f. Hirota, N. and Hutchison, C. A. Jr. (1967). *J. Chem. Phys.*, **46**, 1561
156g. Martin, T. E. and Kalantes, A. H. (1968). *J. Chem. Phys.*, **48**, 4996
156h. Johnson, D., Logan, L. M. and Ross, I. G. (1964). *J. Mol. Spectrosc.*, **14**, 198
157a. Siebrand, W. (1966). *J. Chem. Phys.*, **44**, 4405
157b. Siebrand, W. and Williams, D. F. (1967). *J. Chem. Phys.*, **46**, 403
158. Siebrand, W. (1967). *J. Chem. Phys.*, **46**, 440
159. Murata, S., Iwanaga, C., Toda, T. and Kokubun, H. (1971). *Ber. Bunsenges. Phys. Chem.*, **76**, 1176
160. Kiel, A. (1964). *Quantum Electronics* (P. Grivet and N. Blombergen, editors) Vol. I, p. 765 (New York: Columbia University Press)
161. Riseberg, L. A. and Moos, H. W. (1968). *Phys. Rev.*, **174**, 429
162. Fong, F. K., Naberhuis, S. L. and Miller, M. M. (1972). *J. Chem. Phys.*, **56**, 4020
163. Fong, F. K. and Wassam, W. A. (1973). *J. Chem. Phys.*, **58**, 956
164. Fischer, S. (1971). *Chem. Phys. Lett.*, **11**, 577
165. Nitzan, A. (1974). *J. Chem. Phys.*, in press
166. Brus, L. E. and McDonald, J. R. (1973). *Chem. Phys. Lett.*, **21**, 283
167. Geldof, P. A., Rettschnick, R. P. H. and Hoytink, G. J. (1969). *Chem. Phys. Lett.*, **4**, 59
168. van den Boggardt, P. A. M., Rettschnick, R. P. H., and van Voorst, J. D. W. (1973). *Chem. Phys. Lett.*, **21**, 351
169. Hoytink, G. J. (1973). *Chem. Phys. Lett.*, **22**, 10; (1974). *ibid.*, **26**, 16
170. Wannier, P., Rentzepis, P. M. and Jortner, J. (1971). *Chem. Phys. Lett.*, **10**, 102
171. Wannier, P., Rentzepis, P. M. and Jortner, J. (1971). *Chem. Phys. Lett.*, **10**, 182
172. Busch, G. E., Rentzepis, P. M. and Jortner, J. (1971). *J. Chem. Phys.*, **56**, 361
173. McDonald, J. R. and Bruce, L. E. (1973). *Chem. Phys. Lett.*, **23**, 87
174. Coulson, C. A. and Levine, R. D. (1967). *J. Chem. Phys.*, **47**, 1235